1963

A study of limit design in structural concrete

Wai-Fah Chen
Lehigh University

A STUDY OF LIMIT DESIGN IN

STRUCTURAL CONCRETE

by

Wai-Fah Chen

A THESIS

Presented to the Graduate Faculty

of Lehigh University

in Candidacy for the Degree of

Master of Science

Lehigh University

1963

This thesis is accepted and approved in partial fulfill-ment of the requirements for the degree of Master of Science.

April 24, 1963
(Date)

C. L. Hulsbos
Professor in Charge

W. J. Eney
Professor W.J. Eney, Head
Department of Civil Engineering

ACKNOWLEDGEMENTS

The work described in this thesis was conducted in Fritz Engineering Laboratory of the Department of Civil Engineering, Lehigh University, Bethlehem, Pennsylvania. Professor W.J. Eney is Head of the Department of Civil Engineering and Dr. L.S. Beedle is the Director of Fritz Engineering Laboratory.

The author wishes to acknowledge his gratitude to Professor C.L. Hulsbos, thesis supervisor, for his continued advice, suggestions, and help.

The assistance extended by the author's associates in Fritz Laboratory, especially Messrs. Felicisimo S. Ople, Jr., John M. Hanson and Dick M. Miller, is gratefully acknowledged. Miss Grace Mann typed the manuscript and her patience and cooperation are appreciated.

TABLE OF CONTENTS

Page

LIST OF TABLES

LIST OF FIGURES

1. INTRODUCTION

1.1 Limit Design for Structural Concrete

In recent years, the literature on ultimate strength design has become very extensive. Since 1950, a consolidation of knowledge has been carried out, and new important test data have been published.(1)* Ultimate design theory has been adopted in Russia, Brazil, and several countries in Europe(2) and became a practical reality in the United States with the 1956 ACI Building Code. However, this design theory only takes into account the inelastic behavior of concrete for each individual cross section and it does not consider moment redistribution in the whole structure. Thus, an elastic analysis is still necessary to determine the elastic moment distribution throughout the structure. It would appear to be logical and consistent to use the inelastic design theory for both the whole structure and the individual sections. The theory considering moment redistribution in reinforced concrete structures is referred to as limit design.

1.2 Difference Between Limit Design in Concrete and Plastic Design in Steel

Plastic design theory in steel is based on the principle that a structure will not collapse until sufficient plastic hinges have developed to form it into a mechanism which allows full redistribution

*Numbers placed in such a manner refer to works listed in the references.

of moment. This is possible because the steel has a relatively long plastic region BC as shown in Fig. 1 which is usually adequate to permit each hinge to develop its full plastic moment if the certain factors such as local or lateral buckling or brittle failure are not a problem.(3)

In reinforced concrete, the behavior is different. The long plastic region BC is absent and shortly after any one of the hinges reaches its maximum capacity, complete rupture of the hinge section takes place. As soon as such rupture takes place, the structure may be said to have reached its ultimate capacity irrespective of the total number of plastic sections which may not be sufficient to form the structure into a mechanism. Thus the local rupture of a plastic hinge section prevents the structure from moment redistribution. Therefore, the safe available rotation capacity of the plastic hinge sections in limit design becomes an important factor for the amount of moment redistribution.

1.3 The Effect of Lateral Steel on Concrete Ultimate Strain

It has been shown that the sudden failures observed in concrete compression tests are related to the release of energy stored in the testing machine. By using suitably stiff testing machines, stress-strain relations have been observed beyond the maximum load.(4) An example of such relation observed by the U.S. Bureau of Reclamation is given in Fig. 2. which implies that the ductility of concrete beyond the maximum load is relatively long and can be transformed into a ductile material with constant load by the application of lateral pressure.

This may be accomplished by using sufficient lateral steel in the concrete.[5] Results from bound concrete block tests (Fig. 21b, Fig. 22c) showed that the ultimate strain and the rotation capacity (Fig. 23, Fig. 24) increase considerably without decreasing the ultimate stress.

1.4 Theories of Limit Design

Many theories, such as those of Professor G. C. Ernst,[6] Professor H. A. Sawyer[7] and Professor A. L. L. Baker,[8] have been proposed to determine the required rotation capacity. The most widely applicable theory of limit design so far produced is probably that developed by A.L.L. Baker. Instead of using the general elastic equations of virtual work principle in elastic analysis, he used the following modified equations:

$$
\begin{aligned}
\Delta_{10} + X_1 \Delta_{11} + X_2 \Delta_{12} + \ldots + X_n \Delta_{1n} &= -\theta_1 \\
\Delta_{20} + X_1 \Delta_{21} + X_2 \Delta_{22} + \ldots + X_n \Delta_{2n} &= -\theta_2 \\
\ldots\ldots\ldots\ldots\ldots\ldots\ldots\ldots & \\
\Delta_{no} + X_1 \Delta_{n1} + X_2 \Delta_{n2} + \ldots + X_n \Delta_{nn} &= -\theta_n
\end{aligned}
\qquad (1.1)
$$

where $\Delta_{10}, \Delta_{11}, \Delta_{12} \ldots \Delta_{nn}$ = influence coefficients.

(Δ_{mn} = the rotation of hinge at m due to unit bending moment acting at hinge n in direction X_n in a structure that has become statically determinate by the assumed insertion or formation of sufficient hinges),

$\Delta_{mn} = \int_{str.} \frac{M_m M_n}{EI} ds$ ($\int_{str.}$ indicates a summation over the entire structure.)

M_m = moment at any point in the structure when $X_m = 1$ and all other X's are zero,

$\Delta_{10}, \Delta_{20} \ldots \Delta_{no}$ etc. are the rotations at hinges 1, 2, ... n due to the applied loads when $X_1, X_2 \ldots X_n$ are zero,

M_n = moment at any point in the structure when $X_n = 1$ and all other X's are zero,

$$\Delta_{no} = \int_{str.} \frac{M_n M_o \, ds}{EI}$$

M_O = moment at any point in the structure due to applied loads when X_1, X_2 ... X_n are all zero.

X_m = unknown moment at hinge section m. For elastic conditions equal and opposite unknown bending moments are assumed to act at the hinges, and θ_n must be equal to zero since compatibility condition must be satisfied at the hinge section.

For plastic conditions the known plastic moment of the section is assumed to act at the hinges and remains constant under increasing load. From Eq. (1.1), therefore, the required rotation capacities θ_1, θ_2 ... θ_n etc. may be determined.

Professor Baker suggested a trial-and-adjustment method of design in using these general equations. The method is as follows: the positions of plastic hinges are first assumed and the values of plastic moments X_1, X_2 ... X_n, based on an economical distribution of bending moments are also assumed. Values of θ_1, θ_2 ... θ_n are obtained from the general equations. The positions of the hinges have been correctly chosen if the computed rotations from foregoing equations are positive; if θ's are negative, adjustments must be made to the values of X until the values of θ are positive. The θ values so obtained must be less than the permissible rotations of the hinges; that is, in the hinges the maximum concrete strain must be less than the permissible values. If the concrete strain exceeds the permissible value, lateral steel may be used to increase maximum concrete compression strain or adjustments may be made to the values of X, so that the values of θ are within the permissible range.

The following two major assumptions are made in the application of Eq. (1.1):

(1) The plastic hinges are concentrated at points so that members between hinges remain elastic.

(2) Ultimate load is reached when n plastic hinges form for a structure which is n times statically indeterminate.

Since it is also desirable to avoid excessive deflections and wide cracks under working load, an adequate load factor must be provided in the limit analysis.

1.5 Advantages of Limit Design

Since the members can be reinforced in such a manner that the plastic hinges will be formed at the position chosen, the congestion of reinforcements in one place can then be avoided.

The assumption of plastic hinges in frames can greatly simplify the calculations for structures which are many times statically indeterminate.

Furthermore, the limit analysis of a structure provides a consistent basis between the actual behavior of a structure with its theoretical analysis; a true load factor against structural failure, and the most economical use of materials can be achieved.

1.6 Object and Scope of Thesis

The most widely applicable theory of limit design so far produced is first reviewed in section 1.4. A rapid method of determining the available rotation capacity is developed. Since this method is based on a generalized stress-strain curve for plain and bound concrete, several concrete blocks were tested to obtain some characteristic constants of the assumed curve. Finally the effect of lateral steel ratio on concrete ultimate strain was also obtained from the results of concrete block tests.

2. AVAILABLE HINGE ROTATION CAPACITY

2.1 Introduction

For a given concrete structure, a method of determining the available rotation capacity at each given hinge is developed. In this analytical study, a generalized stress-strain relationship for plain and bound concrete is first proposed, a method based on this relationship for determining the concrete compressive stress factor K_1 and K_2 is then developed, and finally the available hinge rotation capacity is readily computed from the above information.

A numerical example using this method is presented in the Appendix.

2.2 Stress-Strain Relation for Concrete

The generalized stress-strain relationship for concrete as shown in Fig. 3 is used in this study. It consists of a parabola and a sloping straight line. A cubic parabola is used to represent the relation up to ϵ_o and a linear variation is used after ϵ_o.

2.2.1 For $\epsilon < \epsilon_o$

The general cubic equation is expressed in the following form.

$$f = A_1\epsilon^3 + A_2\epsilon^2 + A_3\epsilon + A_4 \tag{2.1}$$

The coefficients of Eq. (2.1) are determined using the following four boundary conditions:

$$\epsilon = 0, \qquad f = 0 \qquad \frac{df}{d\epsilon} = E_c$$

$$\epsilon = \epsilon_o, \qquad f = f''_c \qquad \frac{df}{d\epsilon} = 0$$

Equation (2.1) becomes

$$f = \left(\frac{E_c \epsilon_o - 2f''_c}{\epsilon_o^3} \right) \epsilon^3 + \left(\frac{3f''_c - 2\epsilon_o E_c}{\epsilon_o^2} \right) \epsilon^2 + E_c \epsilon \qquad (2.2)$$

where f =concrete compressive stress

f''_c =maximum concrete compressive stress in flexure

ϵ =unit concrete strain, and

ϵ_o =strain at the stress f''_c.

2.2.2 For $\epsilon > \epsilon_o$

The sloping straight line is expressed in the following form:

$$f = f''_c + \alpha E_c (\epsilon - \epsilon_o) \qquad (2.3)$$

The value α can be determined from experimental tests. It will vary with the amount of lateral steel, characteristics of concrete and many other factors.

The ultimate strain of concrete may be defined as follows:

$$-\alpha E_c \, (\epsilon_u - \epsilon_o) = 0.15 \, f''_c \qquad (2.4)$$

Solving for α we obtain

$$\alpha = \frac{-0.15\ f''_c}{E_c\ (\epsilon_u - \epsilon_o)} \tag{2.5}$$

Substituting Eq. (2.5) into Eq. (2.3),

$$f = f''_c - 0.15\ f''_c\ \frac{(\epsilon - \epsilon_o)}{(\epsilon_u - \epsilon_o)} \tag{2.6}$$

where ϵ_u = ultimate strain of concrete at the stress $0.85\ f''_c$.

2.2.3 Limitation of cubic equation.[9]

If the initial slope is too steep, the cubic parabola reaches a maximum value at a smaller value of ϵ and then becomes a minimum at $\epsilon = \epsilon_o$. It must therefore be stipulated that

$$\frac{d^2f}{d\epsilon^2} \leqslant 0 \qquad \text{at} \qquad \epsilon = \epsilon_o$$

which leads to the result

$$\epsilon_o E_o - 3\ f''_c \leqslant 0$$

$$\frac{\epsilon_o E_c}{f''_c} \leqslant 3 \tag{2.7}$$

2.3 Concrete Compressive Stress Factors K_1, K_2 at Any Stress Stage

The two dimensionless factors K_1 and K_2 are defined as follows:

$$K_1 = \frac{\text{total concrete compressive force}}{bcf''_c}$$

K_2c = distance from extreme compressive fiber to the center of gravity of compressive force in concrete

in which b = width of section

c = distance from extreme compressive fiber to neutral axis.

It is of interest to note that the stress factors K_1 and K_2 so defined will be valid at any stress stage. As the extreme concrete compressive strain ϵ_c reaches its ultimate value ϵ_u, the meaning of K_1 and K_2 at that stress stage will be the same as the meaning commonly used for K_1 and K_2 in ultimate strength design; in other words, the meaning of k_1 and k_2 defined in ultimate strength design is only a special case of the meaning of K_1 and K_2 used in this thesis.

For a rectangular section (see Fig. 4) the values of K_1 and K_2 can then be derived.

The two major assumptions are made:

(1) Linear distribution of strain, and

(2) Concrete compressive stress is a function of strain only, $f = F(\epsilon)$. Effects of other factors are neglected.

Linear strain distribution

$$\frac{\epsilon_c}{c} = \frac{\epsilon_x}{x} \qquad dx = \frac{c}{\epsilon_c} d\epsilon_x$$

Total compressive force = $K_1K_3bcf'_c$

$$= b \int_0^c F(\epsilon_x)\ dx = \frac{bc}{\epsilon_c} \int_0^{\epsilon_c} F(\epsilon_x)d\epsilon_x = \frac{bc}{\epsilon_c} \text{ Area (OAB)}$$

$$K_1 = \frac{\text{Area (OAB)}}{K_3f'_c\epsilon_c} = \frac{\text{Area (OAB)}}{\text{Area (ODCB)}} \tag{2.8}$$

in which $f''_c = K_3f'_c$.

Taking moment about N.A.

$$K_1K_3bcf'_c\ (1-K_2)\ c = b \int_0^c F(\epsilon_x)\ x\ dx = \frac{bc^2}{\epsilon_c^2} \int_0^{\epsilon_c} F(\epsilon_x)\epsilon_x d\epsilon_x$$

$$1 - K_2 = \frac{\int_0^{\epsilon_c} F(\epsilon_x)\ \epsilon_x\ d\epsilon_x}{\epsilon_c^2K_3f'_cK_1} = \frac{\text{Moment area (OAB) about f axis}}{\epsilon_c^2K_3f'_cK_1} \tag{2.9}$$

For a given concrete, K_1, K_2 may be plotted against strain ϵ_c since all the constants are known. A numerical example is presented in the Appendix.

2.4 Numerical Procedure for Plotting K_1, K_2 vs ϵ_c Curves

A simple procedure in plotting these curves may be obtained by the application of numerical approximation. In this approach we first consider the concrete stress-strain curve as an imaginary distributed loading. For an approximation we can convert this distributed loading to a number of equivalent concentrated reactions and K_1, K_2 can be computed from these reactions by using Eq. (2.8) and (2.9).

2.4.1 Equivalent concentrated reaction formulas

A distribution that varies according to the ordinates to an arc of a second degree parabola is sufficiently accurate to represent a cubic curve in a subdivided region. Formulas for the equivalent concentrations for such a load are given in Fig. 5[10] in terms of three ordinates to the load distribution curve. The formulas given in Fig. 5a are for a smooth cubic loading curve and in Fig. 5b for a polygonal Loading curve.

2.4.2 K_1 and equivalent reactions

The stress-strain curve becomes a series of concentrated reactions by using the formulas as shown in Fig. 6.

From Eq.(2.8)

$$\underset{\text{at } \epsilon_1}{K_1} = \frac{A_1}{\lambda_1 K_3 f'_c} \qquad \underset{\text{at } \epsilon_2}{K_1} = \frac{A_1 + A_2}{2} \quad \frac{1}{\lambda_1 K_3 f'_c}$$

$$K_1 = \frac{A_1 + A_2 + A_3}{3} \quad \frac{1}{\lambda_1 \; K_3 \; f'_c} \quad \ldots\ldots \qquad (2.10)$$

in which $A_1 = R_o + R_{1L}$, $A_2 = R_{1R} + R_{2L}$, $A_3 = R_{2R} + R_{3L}$ $\ldots$

2.4.3 K_2 and equivalent reactions

The moments of the areas A_1, $(A_1 + A_2)$, $(A_1 + A_2 + A_3)$ ... about o are as follows:

$$\begin{array}{ll} \text{For } A_1 & R_{1L}\lambda_1 \\ A_1+A_2 & (R_{1L}+R_{1R})\lambda_1 + R_{2L} \cdot 2\lambda_1 \\ A_1+A_2+A_3 & (R_{1L}+R_{1R})\lambda_1 + (R_{2L}+R_{2R})\, 2\lambda_1 + R_{3L} \cdot 3\lambda_1 \\ \ldots & \ldots\ldots\ldots\ldots \end{array} \tag{2.11}$$

By substituting Eq. (2.10) and the quantities (2.11) into Eq. (2.9), the corresponding value of K_2 is determined.

The numerical procedure is much simplified by using a table-type computation form. The same numerical example as used in section 2.3 is presented in Appendix for comparison, and it demonstrates a very good agreement with exact value.

2.5 The Determination of N.A. Location, Kd

Since the stress-strain relationship is generalized for plain and bound concrete and concrete compressive stress factors K_1, K_2 are fully established by the previous method, the stress analysis in reinforced concrete with and without lateral steel becomes a routine procedure by application of equilibrium conditions with the assumption of linear strain variation across the section.

These conditions can be applied to any type of loading and the entire stage of stress history can thus be determined, and the Kd can be determined correspondingly.

2.5.1 Rectangular beam with tension reinforcement only

We obtain by equilibrium of forces and of moments (Fig. 7)

$\Sigma H = 0$

$$0 = K_1 K f_c'' bd - A_s f_s \tag{2.12}$$

ΣM_{A_s}

$$M = K_1 K f_c'' (1-K_2K)\, bd^2 \tag{2.13}$$

Linear strain distribution

$$\frac{\epsilon_c}{K} = \frac{\epsilon_s}{1-K} \qquad \epsilon_s = \epsilon_c \left(\frac{1-K}{K} \right) \tag{2.14}$$

For $\epsilon_s \leqslant \epsilon_y$

$$f_s = E_s \epsilon_s = \epsilon_c E_s \left(\frac{1-K}{K} \right) \tag{2.15}$$

For $\epsilon_s \geqslant \epsilon_y$

$$f_s = f_y \tag{2.16}$$

For a given loading condition, we can assume different values of ϵ_c and find the corresponding concrete compressive stress factors K_1, K_2

from the fully established K_1, K_2 vs ϵ_c curves. The actual unknown values of K and ϵ_c can be determined by trial and error from Eqs. (2.12) to (2.16).

2.5.2 Rectangular beam with compression reinforcements

We also obtain by equilibrium of forces and of moments (Fig. 8):

$\sum H = 0$

$$0 = K_1 \, K f''_c \, bd - A_s f_s + A'_s \, (f'_s - f) \tag{2.17}$$

$\sum M_{As} = 0$

$$M = K_1 \, K f''_c \, (1 - K_2 K) \, bd^2 + A'_s \, (f'_s - f) \, (d - d') \tag{2.18}$$

Linear strain distribution

For $\epsilon'_s \leqslant \epsilon_y$

$$\frac{\epsilon_c}{K} = \frac{\epsilon'_s}{K - d'/d} \qquad f'_s = \epsilon_c E_s \left(\frac{K - d'/d}{K} \right) \tag{2.19}$$

$\epsilon_s \leqslant \epsilon_y$

$$\frac{\epsilon_c}{K} = \frac{\epsilon_s}{1 - K} \qquad f_s = \epsilon_c E_s \left(\frac{1 - K}{K} \right) \tag{2.20}$$

For $\epsilon'_s \geqslant \epsilon_y$, $\epsilon_s \geqslant \epsilon_y$

$$f'_s = f_s = f_y \tag{2.21}$$

Here f = concrete stress corresponding to the strain ϵ_s'. The value of f can be determined from concrete stress-strain relationship as soon as ϵ_c is assumed. Equations(2.17) to (2.21) can be solved by trial and error as in section 2.5.1. In the first trial value it may be better to neglect the small stress f which is the concrete compression stress replaced by compression steel.

2.5.3 Flexure and direct load on rectangular sections

The stress analysis will be exactly the same as in 2.5.1 and 2.5.2. It will not be developed in this thesis.

2.6 Plastic Length L_p

As the load increases towards its ultimate value, the plasticity will develop at the point of maximum stress and extend along the member so that over a short plastic length a large change of slope occurs. We may define the length ending at the section where the tension steel just starts to yield in an under-reinforced section or concrete starts its inelastic behavior in an over-reinforced section. Concrete may be assumed to start its inelastic behavior at a strain equal to 0.001 for most concrete and can be obtained from test results for some special concrete.

Thus, the plastic length L_p can be computed as follows:

$M_{ult.}$ = ultimate moment at the section where plasticity starts first

M_y = yielding moment at the section as defined above where plasticity ends.

Figure 9 shows the free body diagram of the plastic length L_p. The load on this short portion L_p may be neglected.

$$\Sigma M = 0$$

$$L_p = \frac{M_{ult.} - M_y}{V} \qquad (2.22)$$

in which, V = shear force at the plastic hinge. Here V can be readily computed from the member between two plastic hinges.

2.7 Available Rotation Capacity

The angle of discontinuity over the short plastic length is referred to as the rotation of the hinge. To be able to calculate its rotation, the type of plastic hinge must be known. Hinges may be classified as follows:

2.7.1 Tensile plastic hinges

Rotation of a tensile plastic hinge is due mainly to yielding of the tensile steel, accompanied by a rise of neutral axis.

The strain distribution is shown in Fig. 10. (a) is the position of the neutral axis at the commencement of yielding of the steel.

(b) is the position at failure. (c) is the position of the neutral axis for the change of strain in the concrete and is above (b).

As soon as the steel starts to yield, the compatibility condition will not be fulfilled and the redistribution of moment in a member occurs. Therefore the available rotation capacity of a plastic hinge for the moment redistribution is the angle at point (c) as shown in Fig. 11. This angle can be computed as follows:

$$\angle\beta = \angle\alpha - \angle\gamma = \frac{L_p\,\epsilon_{ult.}}{K_u\,d} - \frac{L_p\,\epsilon_e}{Kd} \qquad (2.23)$$

Here

$\angle\alpha$ = total hinge rotation capacity (elastic rotation + plastic rotation)

$\angle\beta$ = plastic rotation capacity, available for moment redistribution. The required value for complete moment redistribution is computed from the modified general elastic equations of virtual work principle.

$\angle\gamma$ = elastic rotation capacity. Compatibility condition of the section at this stage must be fulfilled.

In a bound concrete hinge, the ultimate strain is high in comparison with the elastic strain. Ignoring elastic rotation may not incur serious error.

2.7.2 Compressive plastic hinges

There is no tension in the section, thus the neutral axis is located outside the section.

Available rotation (see Fig. 12)

$$\theta = \frac{(\epsilon_{c_1} - \epsilon_{c_2})}{d} L_p \tag{2.24}$$

The safe available value may be obtained from test results of bound concrete block tests as shown in Figs. 23 and 24. A reasonable safe limiting value for $(\epsilon_{c_1} - \epsilon_{c_2})$ would appear to be 0.005, provided that suitable lateral steel is used as is indicated in the figures.

3. EXPERIMENTAL WORK

3.1 Introduction

The prime purposes of the concrete block tests with different lateral steel ratios were to provide in detail:

(1) verification of the generalized stress-strain relationship for plain and laterally bounded concrete.

(2) determination of the effect of lateral steel ratio on the ultimate strain of concrete.

Three blocks with different lateral steel were tested to failure under an eccentricity of half inch, three with different lateral steel were tested to failure under axial loading. In addition to the block tests with lateral steel, a number of tests were conducted on plain concrete blocks and cylinders to determine the stress-strain properties of the concrete.

3.2 Test Specimens

3.2.1 Materials

(1) Concrete: The concrete was designed to have a 28-day strength of 5000 psi and a slump of 4 inches.

The proportions of the mix by weight were:

Type III portland cement	1.00
Coarse Aggregate (Max. size of 3/4 in.)	3.20

Fine Aggregate	3.30
Water	0.60

The property of the concrete was determined from 6 x 12 in. cylinders. The cylinders were capped with carbo-vitrobond on the top and bottom surfaces. The average stress-strain relationship of the concrete is shown in Figs. 13a and 13b.

(2) Steel: 3/16 in. diameter bars were used as the lateral steel for all blocks. All blocks were longitudinally reinforced with four No. 2 deformed bars. The idealized stress-strain relationship for No. 2 bar is assumed as shown in Fig. 14.

3.2.2 Manufacture

All specimens were cast on their sides in 6 x 6 x 36 in. forms with plates used to divide the forms into three 12 in. lengths. All specimens were stripped at 3 days and cured in a moist room and tested at the end of 28 days.

3.2.3 Details

Details of the specimens tested are given in Table 1, Fig. 15 and Fig. 16.

3.3 Test Procedure

All tests were conducted in the 300,000 lb. hydraulic test machine. The loading was applied through semi-circular pins and thick end plates as shown in Fig. 17.

Strain measurements for the first three specimens were made by using 0.0001 in. Ames dial gages as shown in Fig. 15. All other specimens were measured by using 5 in. Whittemore gages applied at reference points consisting of drilled holes in copper and aluminum lugs which were embeded in the specimens for No. 4, No. 5, and No. 6 as shown in Fig. 16 and were attached with Armstrong's glue on the concrete surface for No. 7. Each specimen had two gage lengths on each face. Deflections were measured for eccentrically loaded specimens at the centroid of less stressed face with 0.0001 in. Ames dial gages.

Loads were added to the specimens in ten kip increments up to 120 kips. As the loading became higher, considerable deformation of concrete occurred and in order to get more accurate stress-strain relationship in this portion the loading increments were gradually reduced to one kip.

The strain of cylinders was measured by compressormeter and they were loaded to failure in 14-16 increments of load.

3.4 Analysis

Stresses can be calculated from the corresponding strain and loading measurements if the following two reasonable assumptions are made:

(1) Linear distribution of strain, and

(2) Concrete stress is a function of strain only, $f = F(\epsilon)$.

3.4.1 N.A. outside the section

From equilibrium of forces and of moments (Fig. 18) we obtain

$$\sum H = 0$$

$$P - A'_s f_{s1} - A_s f_{s2} = b \int_0^t f \, dx = b \int_0^t F(\epsilon_x) dx \qquad (3.1)$$

Using the assumption that plane section remains plane after bending

$$\epsilon_x = \epsilon_{c_2} + \frac{x}{t} (\epsilon_{c_1} - \epsilon_{c_2})$$

$$d\epsilon_x = \frac{\epsilon_{c_1} - \epsilon_{c_2}}{t} dx \qquad (3.2)$$

Substituting (3.2) into (3.1)

$$P - A'_s f_{s1} - A_s f_{s2} = \frac{bt}{\epsilon_{c_1} - \epsilon_{c_2}} \int_{\epsilon_{c_2}}^{\epsilon_{c_1}} F(\epsilon_x) d\epsilon_x \qquad (3.3)$$

Taking moment about 0

$$\sum M_o = 0$$

$$P(e + t/2) - \left[A_s f_{s_2} d' + A'_s f_{s_1} (t-d') \right]$$

$$= b \int_0^t x \, f dx = \frac{bt^2}{(\epsilon_{c_1} - \epsilon_{c_2})^2} \int_{\epsilon_{c_2}}^{\epsilon_{c_1}} (\epsilon_x - \epsilon_{c_2}) F(\epsilon_x) d\epsilon_x \qquad (3.4)$$

For simplicity, denote

$$m_o = P(e + t/2) - \left[A_s f_{s_2} d' + A'_{s_1} f_{s_1} (t-d') \right]$$

$$f_o = P - A'_s f_{s_1} - A_s f_{s_2}$$

Equation (3.3) and (3.4) then reduce to

$$f_o(\epsilon_{c_1} - \epsilon_{c_2}) = bt \int_{\epsilon_{c_2}}^{\epsilon_{c_1}} F(\epsilon_x)\, d\epsilon_x \tag{3.3a}$$

$$m_o(\epsilon_{c_1} - \epsilon_{c_2})^2 = bt^2 \int_{\epsilon_{c_2}}^{\epsilon_{c_1}} (\epsilon_x - \epsilon_{c_2}) F(\epsilon_x)\, d\epsilon_x \tag{3.4a}$$

Differentiate Eq. (3.4a) with respect to ϵ_{c_1}

$$(\epsilon_{c_1} - \epsilon_{c_2})^2 \frac{d\, m_o}{d\, \epsilon_{c_1}} + 2m_o (\epsilon_{c_1} - \epsilon_{c_2}) \left(1 - \frac{d\epsilon_{c_2}}{d\epsilon_{c_1}}\right)$$

$$= bt^2 \frac{d}{d\epsilon_{c_1}} \int_{\epsilon_{c_2}}^{\epsilon_{c_1}} (\epsilon_x - \epsilon_{c_2})\, F(\epsilon_x)\, d\epsilon_x \tag{3.4b}$$

From the theory of integration[11]

$$\frac{d}{d\epsilon_{c_1}} \int_{\epsilon_{c_2}}^{\epsilon_{c_1}} (\epsilon_x - \epsilon_{c_2})\, F(\epsilon_x)\, d\epsilon_x$$

$$= (\epsilon_{c_1} - \epsilon_{c_2})F(\epsilon_{c_1}) - (\epsilon_{c_2} - \epsilon_{c_2})F(\epsilon_{c_2}) - \int_{\epsilon_{c_2}}^{\epsilon_{c_1}} F(\epsilon_x)d\epsilon_x \;\; \frac{d\epsilon_{c_2}}{d\epsilon_{c_1}}$$

$$= (\epsilon_{c_1} - \epsilon_{c_2})\, f_{c_1} - \int_{\epsilon_{c_2}}^{\epsilon_{c_1}} F(\epsilon_x)d\epsilon_x \;\; \frac{d\epsilon_{c_2}}{d\epsilon_{c_1}} \qquad (3.4c)$$

in which

$$f_{c_1} = F(\epsilon_{c_1})$$

Substitute Eq. (3.3a) and (3.4c) into Eq. (3.4b) which finally leads to the result

$$bt^2 f_{c_1} = (\epsilon_{c_1} - \epsilon_{c_2})\, \frac{d\, m_o}{d\epsilon_{c_1}} + 2m_o \left(1 - \frac{d\epsilon_{c_2}}{d\epsilon_{c_1}}\right) + f_o t \;\; \frac{d\epsilon_{c_2}}{d\epsilon_{c_1}}$$

Rearrange

$$bt^2 f_{c_1} = (\epsilon_{c_1} - \epsilon_{c_2})\, \frac{d\, m_o}{d\epsilon_{c_1}} + (f_o t - 2m_o)\, \frac{d\epsilon_{c_2}}{d\epsilon_{c_1}} + 2m_o \qquad (3.5)$$

Differentiate (3.3a) with respect to ϵ_{c_1}

$$\frac{d}{d\epsilon_{c_1}} f_o(\epsilon_{c_1} - \epsilon_{c_2}) = bt \frac{d}{d\epsilon_{c_1}} \int_{\epsilon_{c_2}}^{\epsilon_{c_1}} F(\epsilon_x)\, dx$$

$$= bt \left[F(\epsilon_{c_1}) - F(\epsilon_{c_2}) \frac{d\epsilon_{c_2}}{d\epsilon_{c_1}} \right] = bt \left[f_{c_1} - f_{c_2} \frac{d\epsilon_{c_2}}{d\epsilon_{c_1}} \right] \quad (3.3b)$$

After cracking occurs, $f_{c_2} = 0$, from Eq. (3.3b)

$$bt\, f_{c_1} = \frac{d}{d\epsilon_{c_1}} f_o(\epsilon_{c_1} - \epsilon_{c_2}) \quad (3.6)$$

From Eq. (3.3b) associated with Eq. (3.5)

$$bt^2 f_{c_2} = (\epsilon_{c_1} - \epsilon_{c_2}) \frac{d\, m_o}{d\epsilon_{c_2}} + 2m_o \frac{d\epsilon_1}{d\epsilon_2} + (f_o t - 2m_o) - \frac{d}{d\epsilon_{c_2}} f_o(\epsilon_{c_1} - \epsilon_{c_2}) \quad (3.7)$$

3.4.2 N.A. inside the section

It is assumed that concrete stress is a function of strain only and that the stress function is the same for tension and compression, i.e. $F(-\epsilon_x) = -F(\epsilon_x)$. From equilibrium of forces and of moments (see Fig. 19), we obtain

$\sum H = 0$

$$P - A'_s f_{s_1} + A_s f_{s_2} = b \left[\int_o^c F(\epsilon_x)\, dx - \int_o^{t-c} F(\epsilon_x)\, dx \right] \quad (3.8)$$

The plane section remains plane after bending,

$$\epsilon_x = \frac{\epsilon_c}{c}\, x = \frac{\epsilon_t}{t-c}\, x$$

$$d\epsilon_x = \frac{\epsilon_c}{c}\, dx = \frac{\epsilon_t}{t-c}\, dx \tag{3.9}$$

Substituting Eq. (3.9) into Eq. (3.8)

$$P - A'_s f_{s_1} + A_s f_{s_2} = b \left[\frac{c}{\epsilon_c} \int_o^{\epsilon_c} F(\epsilon_x)\, d\epsilon_x - \frac{t-c}{\epsilon_x} \int_o^{\epsilon_t} F(\epsilon_x)\, d\epsilon_x \right] \tag{3.10}$$

Taking moment about N.A. and associated with Eq. (3.9)

$$\sum M_{N.A.} = 0$$

$$P(e + c - \frac{t}{2}) - A'_s f_{s_1} (c-d') - A_s f_{s_2} (t - c - d')$$

$$= b \left[\int_o^{c} xfdx + \int_o^{t-c} xfdx \right]$$

$$= \frac{bc^2}{\epsilon_c^2} \left[\int_o^{\epsilon_c} \epsilon_x F(\epsilon_x)\, d\epsilon_x + \int_o^{\epsilon_t} \epsilon_x F(\epsilon_x)\, d\epsilon_x \right] \tag{3.11}$$

For simplicity, denote

$$bcf'_o = P - A'_s f_{s_1} + A_s f_{s_2}$$

$$bc^2 m'_o = P\,(e + c - t/2) - A'_s f_{s_1} (c - d') - A_s f_{s_2} (t - c - d')$$

Eq. (3.10) and (3.11) then reduce to

$$f'_o = \frac{1}{\epsilon_c}\left[\int_o^{\epsilon_c} F(\epsilon_x)\, d\epsilon_x - \int_o^{\epsilon_t} F(\epsilon_x)\, d\epsilon_x\right] \tag{3.10a}$$

$$m'_o = \frac{1}{\epsilon_c^2}\left[\int_o^{\epsilon_c} \epsilon_x F(\epsilon_x)\, d\epsilon_x + \int_o^{\epsilon_t} \epsilon_x F(\epsilon_x)\, d\epsilon_x\right] \tag{3.11a}$$

Differentiate Eqs. (3.10a) and (3.11a) with respect to ϵ_c

$$\epsilon_c \frac{d\, f'_o}{d\, \epsilon_c} + f'_o = f_c - f_t \frac{d\, \epsilon_t}{d\, \epsilon_c} \tag{3.10b}$$

$$\epsilon_c^2 \frac{d\, m'_o}{d\, \epsilon_c} + 2m'_o\epsilon_c = \epsilon_c f_c + \epsilon_t f_t \frac{d\, \epsilon_t}{d\, \epsilon_c} \tag{3.11b}$$

in which

$$f_c = F(\epsilon_c) \qquad \text{and} \qquad f_t = F(\epsilon_t)$$

Eliminate $\frac{d\, \epsilon_t}{d\, \epsilon_c}$ between Eqs. (3.10b) and (3.11b)

$$(\epsilon_c + \epsilon_t)\, f_c = \epsilon_c^2 \frac{d\, m'_o}{d\, \epsilon_c} + 2m'_o\epsilon_c + \epsilon_c\epsilon_t \frac{d\, f'_o}{d\, \epsilon_c} + f'_o\epsilon_t$$

Rearranging finally leads to the result

$$f_c = \frac{1}{(\epsilon_c + \epsilon_t)}\left[\epsilon_c^2 \frac{dm'_o}{d\, \epsilon_c} + 2m'_o\epsilon_c + \epsilon_c\epsilon_t \frac{d\, f'_o}{d\, \epsilon_c} + f'_o\epsilon_t\right] \tag{3.12}$$

After cracking occurs, $f_t = 0$, from Eq. (3.10b)

$$f_c = \epsilon_c \frac{d f'_o}{d \epsilon_c} + f'_o = \frac{d}{d\epsilon_c} (\epsilon_c f'_o) = \frac{d}{d\epsilon_c} (\frac{\epsilon_c f_o}{bc}) \tag{3.13}$$

Here f_o is defined in section 3.4.1 as $f_o = P - A'_s f_{s_1} - A_s f_{s_2}$ assuming tension is negative in f_o, we have $f'_o = \frac{f_o}{bc}$. By substituting (see Eq. (3.9))

$$c = \frac{\epsilon_c t}{\epsilon_t + \epsilon_c}$$

into Eq. (3.13), we obtain

$$btf_c = \frac{d}{d \epsilon_c} (\epsilon_t + \epsilon_c) f_o \tag{3.14}$$

Using $\epsilon_t = -\epsilon_{c_2}$, $\epsilon_c = \epsilon_{c_1}$ and $f_c = f_{c_1}$ as in comparison with Eq.(3.6), these two equations are identical.

3.4.3 Application of these formulae

Equations (3.5), (3.6), (3.7), (3.12), and (3.14) give concrete stress as a function of the continuously measured strain, loading, deflection and specimen's dimensions. The differentials may be closely approximated by finite differences.

It should be noted that the eccentricity e used in these formulas should include the deflections of tested specimens measured in the tests.

3.5 Test Results

3.5.1 Stress-strain curves

By assuming that strain is distributed linearly, the strain relationship between the measuring dial gages and the strains at the specimen surfaces as well as the strains at reinforced bars can be easily established as shown in Fig. 20.

From the figure

$$\epsilon_{c_1} = \epsilon'_{c_2} + 0.8\ (\epsilon'_{c_1} - \epsilon'_{c_2})$$

$$\epsilon_{c_2} = \epsilon'_{c_2} + 0.2\ (\epsilon'_{c_1} - \epsilon'_{c_2})$$

$$\epsilon_{s_1} = \epsilon'_{s_2} + 0.75\ (\epsilon'_{c_1} - \epsilon'_{c_2})$$

$$\epsilon_{s_2} = \epsilon'_{c_2} + 0.25\ (\epsilon'_{c_1} - \epsilon'_{c_2})$$

and also,

$$\epsilon_y = 0.002 \text{ in./in.} \qquad A_s = A'_s = 2 \times 0.05 \text{ in.}^2 = 0.10 \text{ in.}^2$$

$$E_s = 30 \times 10^3 \text{ ksi.} \qquad f_y = 60 \text{ ksi}$$

For $\epsilon_s \leqslant \epsilon_y$

$$A'_s f_{s_1} = 0.1 \times 30 \times 10^3\ \epsilon_{s_1} = 3 \times \epsilon_{s_1} \times 10^3$$

$$A_s f_{s_2} = 0.1 \times 30 \times 10^3\ \epsilon_{s_2} = 3 \times \epsilon_{s_2} \times 10^3$$

From above information, the m_o and f_o can be computed for each load stage.

$$m_o = P(e + \frac{t}{2}) - \left[A_s f_{s_2} d' + A'_s f_{s_1} (t - d') \right]$$

$$f_o = P - A'_s f_{s_1} - A_s f_{s_2}$$

and m_o, f_o, ϵ_{c_2} vs ϵ_{c_1} are plotted as shown in Figs. 21a and 22a. By finite differences $\frac{\Delta m_o}{\Delta \epsilon_{c_1}}$ and $\frac{\Delta \epsilon_{c_2}}{\Delta \epsilon_{c_1}}$ are obtained from the graphic curves, Eq. (3.5) then can be used to derive complete stress-strain relationship for bound concrete in flexure. The stress-strain curves obtained are shown in Fig. 21b and Fig. 22c.

It should be noted that when cracking occurs, Eq. (3.6) should be used instead of Eq. (3.5). Thus $f_o(\epsilon_{c_1} - \epsilon_{c_2})$ vs ϵ_{c_1} is plotted as shown in Fig. 22b and the same procedure is followed. When tension is occurring in the section before cracking, Eq. (3.12) may be used for a more accurate analysis during such loading stages.

3.5.2 Rotation characteristics

Two typically characteristic rotation curves are shown in Fig. 23 and Fig. 24 and the special values of strains in concrete and reinforced bars are self-explained in the figures.

3.5.3 Deflection curves

The center deflections of each specimen have been used as a modified eccentricity in computing stress-strain relationship for section 3.5.1. One of the three deflection curves is shown in Fig. 25.

3.5.4 The effect of lateral steel ratio to ultimate strain in concrete

The relationship between lateral steel ratio and ultimate strain in concrete is shown in Fig. 26. Here the lateral steel ratio is given by

$$P_{\ell} = \frac{\text{Volume of total lateral steel}}{\text{Volume of total concrete}}$$

3.6 Conclusions

A rapid method of determining the available rotation capacity is developed in Chapter 2. This method is based on a generalized stress-strain relationship for plain and bound concrete which is shown from the tests to be sufficiently accurate.

Concrete deformation is considerably limited by brittleness and tests show that lateral steel can increase its ductile ability, (Fig. 22c) providing it with a considerable long horizontal plastic deformation without decreasing the net stress. This is very helpful in the development of limit design theory in concrete structures.

The initial moduli of elasticity and ultimate stress of concrete obtained from plain concrete blocks, and lateral bound blocks were essentially the same.

4. APPENDIX - SAMPLE CALCULATION

4.1 K_1, K_2 vs ϵ_c Curves (Exact Method)

4.1.1 Properties of the concrete

$$\epsilon_o = 0.003, \quad \frac{E_c}{f''_c} = 1000, \quad \alpha = 0$$

$$(K_3 = 1, \quad f''_c = K_3 f'_c = f'_c)$$

From Eq. (2.7), we obtain

$$\frac{\epsilon_o E_c}{f''_c} = 3 \tag{4.1}$$

4.1.2 For $\epsilon \leqslant \epsilon_o$

The generalized stress-strain curve for the concrete is obtained by the substitution of the values in section 4.1.1 into Eq. (2.2).

$$\frac{f}{f''_c} = \frac{10^9}{27}\epsilon^3 - \frac{10^6}{3}\epsilon^2 + 10^3\epsilon \tag{4.2}$$

Area (OAB) (see Fig. 4), bounded by the generalized curve and ϵ-axis, is then obtained by integration.

$$\text{Area (OAB)} = \int_0^{\epsilon_c} f \, d\epsilon_x$$

$$= f''_c \int_0^{\epsilon_c} \left(\frac{10^9}{27}\epsilon_x^{\,3} - \frac{10^6}{3}\epsilon_x^{\,2} + 10^3 \epsilon_x \right) d\epsilon_x$$

$$= 10^3 \epsilon_c^{\,2} f''_c \; \frac{54 - (12)\, 10^3 \epsilon_c + 10^6 \epsilon_c^{\,2}}{108}$$

Area (ODCB) = $\epsilon_c f''_c$

From Eq. (2.8), we obtain

$$K_1 = \frac{\text{Area (OAB)}}{\text{Area (ODCB)}}$$

$$= \frac{54 - (12)\, 10^3\, \epsilon_c + 10^6\, \epsilon_c^{\ 2}}{108}\, 10^3 \epsilon_c \qquad (4.3)$$

Moment area (OAB) about the f axis is also obtained by integration.

$$\text{Moment area (OAB)} = f''_c \int_o^{\epsilon_c} \frac{f}{f''_c}\, \epsilon_x\, d\epsilon_x$$

$$= f''_c \int_o^{\epsilon_c} \left(\frac{10^9}{27}\, \epsilon_x^{\ 4} - \frac{10^6}{3}\, \epsilon_x^{\ 3} + 10^3\, \epsilon_x^{\ 2} \right) d\epsilon_x$$

$$= \frac{10^3 \epsilon_c^{\ 3} f''_c}{3} \cdot \frac{180 - (45)\, 10^3\, \epsilon_c + (4)\, 10^6\, \epsilon_c^{\ 2}}{180}$$

From Eq. (2.9), we obtain

$$1 - K_2 = \frac{\text{Moment area (OAB) about f axis}}{\epsilon_c^{\ 2}\, K_3\, f'_c\, K_1}$$

$$= \frac{\left[180 - (45)\, 10^3\, \epsilon_c + (4)\, 10^6\, \epsilon_c^{\ 2}\right] 10^3 \epsilon_c}{540\, K_1} \qquad (4.4)$$

At the strain $\epsilon_c = \epsilon_o = 0.003$, we have

$K_1 = 3/4 = 0.75$

$K_2 = 1 - 0.6 = 0.4$

4.1.3 For $\epsilon \geqslant \epsilon_o$

Area (OEG) (See Fig. 4) and its moment area about the f-axis are determined by the same procedure as discussed in section 4.1.2.

$$\text{Area (OEG)} = \text{Area (OAB)}_{\text{at } \epsilon_c = \epsilon_o} + (\epsilon_c - \epsilon_o)\, f''_c$$

$$= (2.25)\ 10^{-3}\ f''_c + \left[\epsilon_c - (3)\ 10^{-3}\right] f''_c$$

$$= \epsilon_c f''_c - (0.75)\ 10^{-3}\ f''_c$$

$$\text{Area (OEFD)} = \epsilon_c f''_c$$

Substituting into Eq. (2.8), we obtain

$$K_1 = \frac{\text{Area (OEG)}}{\text{Area (OEFD)}} = 1 - \frac{(0.75)\ 10^{-3}}{\epsilon_c} \tag{4.5}$$

Moment area (OEG) about the f-axis

$$= \left.\begin{array}{l}\text{Moment area (OAB)}\\ \text{about f-axis}\end{array}\right|_{\text{at } \epsilon=\epsilon_o} + (\epsilon_c - \epsilon_o) f''_c \left(\epsilon_o + \frac{\epsilon_c - \epsilon_o}{2}\right)$$

$$= (1 - K_2)\epsilon_c^{\,2} f''_c K_1 \Big|_{\text{at } \epsilon=\epsilon_o} + (\epsilon_c - \epsilon_o) f''_c \left(\epsilon_o + \frac{\epsilon_c - \epsilon_o}{2}\right)$$

$$= (1 - 0.4)\ (9)\ 10^{-6}\ (0.75)\ f''_c + \frac{1}{2}(\epsilon_c^{\,2} - \epsilon_o^{\,2})\ f''_c$$

$$= (4.05)\ 10^{-6}\ f''_c + \frac{1}{2}\epsilon_c^{\,2} f''_c - (4.5)\ 10^{-6}\ f''_c$$

$$= 0.5\ \epsilon_c^{\,2} f''_c - (0.45)\ 10^{-6}\ f''_c$$

Substituting into Eq. (2.9), we obtain

$$1 - K_2 = \frac{\text{Moment area (OEG) about f-axis}}{\epsilon_c^2 \ f''_c \ K_1}$$

$$= \frac{0.5\ \epsilon_c^2\ f''_c - (0.45)\ 10^{-6}\ f''_c}{\epsilon_c^2\ f''_c\ K_1}$$

$$= \frac{\epsilon_c^2 - (0.9)\ 10^{-6}}{2\ \epsilon_c^2\ K_1} \qquad (4.6)$$

4.1.4 The stress factors K_1, K_2 can be plotted against concrete strain ϵ_c, since they are now expressed as a function of ϵ_c alone. The curves obtained from Eqs. (4.3), (4.4), (4.5) and (4.6) are plotted in Fig. 27 and some corresponding values are tabulated in Table 2.

4.2 K_1 K_2 vs ϵ_c Curves (Numerical Approximation)

Details of the table-type computation for stress factors K_1, K_2 vs ϵ_c are given in Table 3. The curves are also plotted in Fig. 27 as dotted-line curves which show very good agreement with exact values (see Table 2).

4.3 Ø vs M Curve for a Rectangular Beam with Tension Reinforcements Only

4.3.1 Given

$E_s = 30 \times 10^6$ psi, $\quad p = 0.02, \quad \epsilon_y = 0.001$

$f'_c = 5000$ psi $\quad (f''_c = K_3 f'_c,\ K_3 = 1)$

4.3.2 For $\epsilon_s \leq \epsilon_y$

From Eq. (2.13), we obtain

$$\frac{M}{f''_c\ bd^2} = K_1\ K(1 - K_2\ K) \tag{4.7}$$

Solving Eq. (2.12) for K and making the substitution for f_s from Eq. (2.15) lead to the result

$$K = \frac{pm\epsilon_c}{2\ K_1}\left(-1 \pm \sqrt{1 + \frac{4\ K_1}{pm\epsilon_c}}\right) \tag{4.8}$$

where

$$m = \frac{E_s}{f''_c}, \quad p = \frac{A_s}{bd}$$

Substituting the given values in section 4.3.1 into Eq. (4.8), we obtain

$$K = \frac{60\ \epsilon_c}{K_1}\left(-1 + \sqrt{1 + \frac{K_1}{30\epsilon_c}}\right) \tag{4.9}$$

4.3.3 For $\epsilon_s \geq \epsilon_y$

Solving Eq. (2.12) for K and substituting the given values from section 4.3.1 into it we obtain

$$K = \frac{A_s f_y}{K_1 f''_c bd} = \frac{pf_y}{K_1 f''_c} = \frac{0.12}{K_1} \tag{4.10}$$

4.3.4 Using the curves in Fig. 27, the corresponding values of K_1 and K_2 are determined for different values of ϵ_c. Substituting these values of K_1 and K_2 into Eqs. (4.7), (4.9), or (4.10), the values of K and M are obtained for different values of ϵ_c. Some of these results are tabulated in Table 4. The steel strain ϵ_s is also listed in the Table. The K vs ϵ_c and M vs ϵ_c curves are plotted in Fig. 28.

At $\epsilon_s = \epsilon_y$, we have

$$M = M_y = 0.1045\ f'_c\ bd^2$$

At $\epsilon_c \rightarrow \infty$, we have

$$M = M_{\epsilon_c \rightarrow \infty} = 0.113\ f'_c\ bd^2$$

4.3.5 Ultimate moment (by the 1956 ACI Building Code)

From the Code, we have

$$M_{ult.} = bd^2\ f'_c\ q\ (1 - 0.59\ q) \tag{4.11}$$

where

$$q = pf_y/f'_c = 0.02\ \frac{(0.001)\ (30)(10^6)}{5000} = \frac{6}{50}$$

Substituting the value of q into Eq. (4.11), we obtain

$$M_{ult.} = bd^2 f'_c\ \frac{6}{50}\left[1 - \frac{(0.59)6}{50}\right] = 0.1114\ bd^2 f'_c$$

This ultimate moment calculated by the Code is in good agreement with the two values shown in section 4.3.4 since it falls between M_y and $M_{\epsilon_c \rightarrow \infty}$

4.3.6 $\emptyset$ vs M curve

For non-dimensional plot denote

$$\emptyset = \text{curvature} = \frac{\epsilon_c}{Kd}$$

$$\emptyset_y = \text{curvature (at } \epsilon_s = \epsilon_y)$$

$$= \frac{\epsilon_e}{(Kd)_{\text{at } \epsilon_s = \epsilon_y}}$$

where

$$\epsilon_e = \text{corresponding concrete strain } \epsilon_c \text{ at } \epsilon_s = \epsilon_y$$

From Table 4, we obtain $\epsilon_e = 0.7 \times 10^{-3}$ and $K = 0.407$ at $\epsilon_s = \epsilon_y = 0.001$. Thus,

$$\emptyset_y = \frac{(0.7)\ 10^{-3}}{0.407\ d} = \frac{(1.72)\ 10^{-3}}{d}$$

and

$$\frac{\emptyset}{\emptyset_y} = \frac{\epsilon_c}{(1.72)\ 10^{-3}\ K} \qquad (4.12)$$

The values of $\emptyset/\emptyset_y$ corresponding to different values of ϵ_c are also tabulated in Table 4. The $M/f_c'bd^2$ vs $\emptyset/\emptyset_y$ curve is then plotted in Fig. 28.

4.4 Plastic Length L_p

Use $M_{ult.} = 0.1114\ f_c'\ bd^2$

$$M_y = 0.1045\ f_c'\ bd^2 \text{ (see Table 4 at } \epsilon_s = \epsilon_y)$$

Assuming uniform load w along the member, we have, (see Fig. 29)

$$V = \frac{wL}{2}$$

$$M = \frac{1}{8} wL^2 = 2M_{ult.}$$

$$wL^2 = 16 M_{ult.} = 1.78 f'_c bd^2$$

Substituting these values into Eq. (2.22), we obtain

$$L_p = \frac{M_{ult.} - M_y}{V} = \frac{0.0069 f'_c bd^2}{\frac{1}{2} wL} = \frac{L}{130}$$

where

L = length of the member between two plastic hinges

V = shear force at the hinges.

4.5 Available Rotation Capacity

Use

$$\epsilon_{ult.} = 0.003$$

$\epsilon_e = 0.0007$ (see Table 4 at $\epsilon_s = \epsilon_y$)

$K = 0.407$ = constant corresponding to ϵ_e
(see Table 4 at $\epsilon_s = \epsilon_y$)

$K_u = 0.16$ = constant corresponding to $\epsilon_{ult.}$
(see Table 4 at $\epsilon_c = 0.003$)

From Eq. (2.23) (See Fig. 11)

$$\angle\beta = \angle\alpha - \angle\gamma = \frac{L_p \epsilon_{ult.}}{K_u d} - \frac{L_p \epsilon_e}{Kd}$$

$$= \frac{L_p \epsilon_{ult.}}{K_u d} \left(1 - \frac{\epsilon_e}{\epsilon_{ult.}} \cdot \frac{K_u}{K} \right)$$

$$= 0.908 \frac{L_p \epsilon_{ult.}}{K_u d} \tag{4.13}$$

If the elastic rotation is neglected, i.e. the second term in Eq. (4.13) is neglected, the error involved is about 10% on the unsafe side in this particular example. If the hinge is bounded with sufficient lateral steel, the concrete ultimate strain may increase to 0.01, then the second term $\frac{\epsilon_e}{\epsilon_{ult.}} = \frac{0.0007}{0.01} = 0.07$, and the error is about 2%.

4.6 Required Rotation Capacity

A continuous beam subject to bending moments due to a load as shown at M_o in Fig. 30 where the plastic hinges are assumed to occur at the supports. Bending moments are plotted on the tensile side of the beams and for each hinges as shown at M_1 and M_2 in Fig. 30. The general Baker's equations give (see Eq. (1.1)).

$$\Delta_{10} + X_1\Delta_{11} + X_2\Delta_{12} = -\theta_1$$

$$\Delta_{20} + X_1\Delta_{21} + X_2\Delta_{22} = -\theta_2$$

Graphic integration gives

$$\Delta_{10} = \frac{2}{EI}\left[\quad\right] = -\frac{2}{3}\frac{ML}{EI}$$

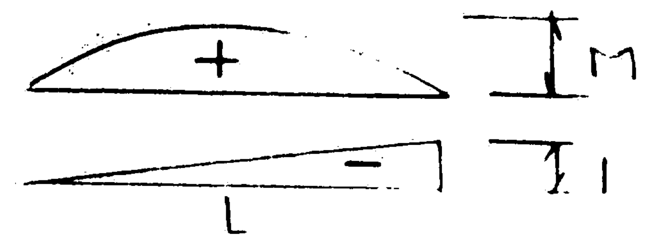

$$\Delta_{20} = \frac{2}{EI}\left[\quad\right] = -\frac{2}{3}\frac{ML}{EI}$$

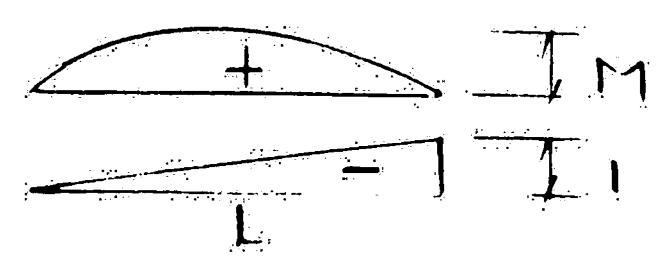

$$\Delta_{11} = \frac{1}{EI}\left[\quad\right] = \frac{2}{3}\frac{L}{EI}$$

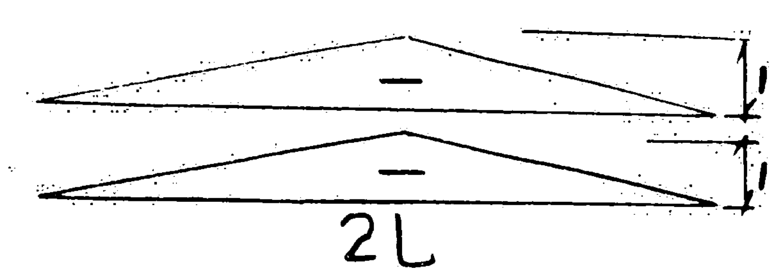

$$\Delta_{22} = \frac{1}{EI}\left[\quad\right] = \frac{2}{3}\frac{L}{EI}$$

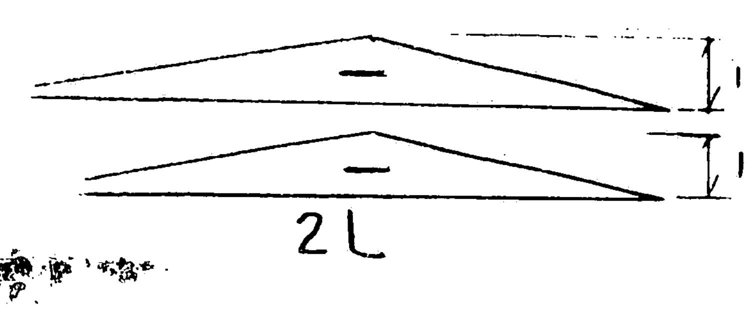

$$\Delta_{12} = \Delta_{21} = \frac{1}{EI}\left[\quad\right] = \frac{1}{6}\frac{L}{EI}$$

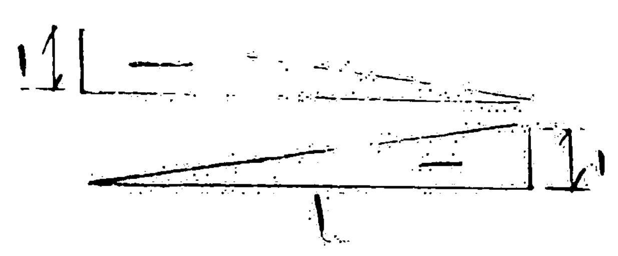

For an economical bending moment distribution throughout the beam, we choose

$$X_1 = X_2 = \frac{M}{2}$$

Substituting Δ_{mn} and X into Baker's general equations, we obtain

$$-\frac{2}{3}\frac{ML}{EI} + \frac{2}{3}\frac{L}{EI}\frac{M}{2} + \frac{1}{6}\frac{L}{EI}\frac{M}{2} = -\theta_1$$

$$-\frac{2}{3}\frac{ML}{EI} + \frac{1}{6}\frac{L}{EI}\frac{M}{2} + \frac{2}{3}\frac{L}{EI}\frac{M}{2} = -\theta_2$$

which leads to the result

$$\theta_1 = \frac{1}{4}\frac{ML}{EI}$$

$$\theta_2 = \frac{1}{4}\frac{ML}{EI}$$

All values of θ are positive. The positions of the hinges have therefore been correctly chosen. The hinge sections must be checked to ensure that the rotations ML/4EI can develop without failure which will be discussed in detail in section 4.7. In general, the required rotation capacity may be written in the following generalized form.

$$\theta_{req.} = \frac{ML}{aEI}$$

where

a = constant (may be determined from Eq. (1.1)).

4.7 Required Rotation Vs. Available Rotation Capacity

Given:

$$\text{Required rotation} = \frac{M_{ult.}}{a\,E_c I}$$

(Using $M = M_{ult.}$)

$$\frac{E_c}{f''_c} = 1000 \qquad (K_3 = 1,\ f''_c = K_3 f'_c = f'_c)$$

$$I = \frac{bd^3}{12}$$

$$L_p = XL$$

$$M_{ult.} = 0.111\ f'_c bd^2 \quad (\text{See Table 4 at } \epsilon_c = 0.0015)$$

$K_u = 0.225$ (See Table 4 at $\epsilon_c = 0.0015$)

$\epsilon_e = 0.0007$ (See Table 4 at $\epsilon_s = \epsilon_y$)

$K = 0.407$ (See Table 4 at $\epsilon_s = \epsilon_y$)

Available Rotation = Required Rotation

$$\frac{\epsilon_u L_p}{K_u d} - \frac{\epsilon_e L_p}{Kd} = \frac{M_{ult.} L}{aE_c I} \tag{4.14}$$

Substituting the given values into Eq. (4.14) we obtain

$$\frac{\epsilon_u XL}{0.225d} - \frac{0.0007\ XL}{0.407d} = \frac{0.111 f'_c\ bd^2\ 12L}{a\ E_c\ bd^3}$$

$$= \frac{(1.332)\ (10^{-3})\ L}{ad}$$

Rearrange,

$$a\ X \left[\epsilon_u - (0.387)\ 10^{-3}\right] = (0.3)\ 10^{-3}$$

If $a = 4$, which usually gives a high value of required rotation, and $\epsilon_u = 0.0015$ then $X = 0.0674 \doteq 1/15$. If X is too high, lateral steel may be provided to increase the ultimate strain of concrete and thus correspondingly decrease the plastic length L_p. The safe limiting value of L_p as was investigated by Professor Baker is about equal to d where d is the effective depth of beam.

5. NOMENCLATURE

a = Constant defined in section 4.6

ϵ = Concrete strain

ϵ_o = Concrete strain at the stress f''_c

$\epsilon_{ult.}$ = Concrete strain at ultimate

ϵ_{c1} = Concrete strain at the most stressed face

ϵ_{c2} = Concrete strain at the less stressed face

f_o, m_o = Defined in section 3.4.1

f'_o, m'_o = Defined in section 3.4.2

f = Concrete compressive stress

f''_c = Maximum concrete compressive stress in flexure

K_1, K_2 = Concrete compressive stress factors defined in section 2.3

L_p = Plastic length defined in section 2.6

V = Shear force at the hinges

Δ_{mn} = Influence coefficients

X_m = Unknown moments at hinge section m

θ = Hinge rotation

α = Concrete characteristic constant defined in Eq. (2.5)

6. TABLES AND FIGURES

Table 1 OUTLINE OF TESTS

No.	Size	Reinforcement		Lateral Steel			Eccentricity	Remarks
		A'_s (in. dia)	A_s (in. dia)	Dia. (in.)	Pitch (in.)	Total No. (N)	(e)	
1	6" x 6" x 12"	$2 \times \frac{1}{4}$	$2 \times \frac{1}{4}$	$\frac{3}{16}$	1	12	$\frac{1}{2}$ in.	$\frac{1}{2}$ in. cover
2	6" x 6" x 12"	$2 \times \frac{1}{4}$	$2 \times \frac{1}{4}$	$\frac{3}{16}$	$1\frac{1}{2}$	8	$\frac{1}{2}$ in.	
3	6" x 6" x 12"	$2 \times \frac{1}{4}$	$2 \times \frac{1}{4}$	$\frac{3}{16}$	2	6	$\frac{1}{2}$ in.	
4	6" x 6" x 12"	$2 \times \frac{1}{4}$	$2 \times \frac{1}{4}$	$\frac{3}{16}$	$2\frac{1}{2}$	5	0	
5	6" x 6" x 12"	$2 \times \frac{1}{4}$	$2 \times \frac{1}{4}$	$\frac{3}{16}$	$3\frac{2}{3}$	4	0	
6	6" x 6" x 12"	$2 \times \frac{1}{4}$	$2 \times \frac{1}{4}$	$\frac{3}{16}$	$5\frac{1}{2}$	3	0	
7	6" x 6" x 12"	None	None	None	None	0	0	Total 3 Blocks
8	6x12" Cyl.	None		None		None	0	Total 7 Cyl.

Table 2 VALUES OF K_1, K_2 vs ϵ_c (BY EXACT METHOD)

K \ $\epsilon_c \times 10^{-3}$	0.5	1.0	1.5	2.0	2.5	3.0	3.5	6.0
K_1	0.223	0.398	0.532	0.630	0.706	0.750	0.785	0.875
K_2	0.343	0.353	0.367	0.377	0.394	0.400	0.409	0.444

Table 3 NUMERICAL APPROXIMATION IN COMPUTING K_1, K_2 vs ϵ_c CURVES

ϵ_c	0	0.001	0.002	0.003	0.004	0.005	Common Factors	Remarks*
f	0	0.704	0.964	1.000	1.000	1.000	f''_c	(1)
R	3.250	6.080 9.930	10.750 13.340	11.940 12.070	12.000 12.000	12.000 12.000	$\frac{\lambda f''_c}{24}$	(2)
A	9.33	(16) 20.68	(24) 25.28	(24) 24.07	(24) 24.00		$\frac{\lambda f''_c}{24}$	(3)
$\sum A$	9.33	30.01	55.29	79.36	103.36		$\frac{\lambda f''_c}{24}$	(4)
K_1	0	0.389	0.627	0.768	0.827	0.862	-	(5)
$A\bar{\epsilon}$		6.08	(16) 37.50	(48) 99.00	(72) 184.20	(96) 292.20	$\frac{\lambda^2 f''_c}{24}$	(6)
$1-K_2$	0	0.652	0.624	0.597	0.571	0.565	-	(7)
K_2	0	0.342	0.374	0.401	0.429	0.435	-	(8)

Note: The same numerical example as used in section 4.1 is presented here for comparison.

*See next page.

Table 3 - Continued

Remarks:

(1) The generalized stress-strain curve for given concrete is obtained in section 4.1.2 (see Eq. (4.2)).

$$\frac{f}{f''_c} = \frac{10^9}{27} \epsilon^3 - \frac{10^6}{3} \epsilon^2 + 10^3 \epsilon \qquad (\epsilon \leq \epsilon_o)$$

$$\frac{f}{f''_c} = 1 \qquad (\epsilon \geq \epsilon_o)$$

The value of f is obtained by substituting the corresponding values of ϵ_c into above equations.

(2) Equivalent reactions are obtained by using the formulas as given in Fig. 5 (here, $\lambda = 0.001$).

(3), (4), (5). By the application of Eq. (2.10) in section 2.4.2.

(6), (7), (8). By the application of Eqs. (2.9), (2.11) in sections 2.3 and 2.4.3.

Table 4. VALUES OF K, $M/f'_c bd^2$, ϕ/ϕ_y and ϵ_s VS ϵ_c

ϵ_c	0.0002	0.0004	0.0006	0.0007	0.0009	0.0015	0.003	∞
K_1	0.100	0.190	0.260	0.300	0.370	0.535	0.750	1.000
K_2	0.340	0.345	0.350	0.351	0.355	0.370	0.400	0.500
K	0.384	0.392	0.406	0.407	0.325	0.225	0.160	0.120
$\frac{M}{f'_c bd^2}$	0.0334	0.0644	0.0908	0.1045	0.1065	0.1110	0.1125	0.1130
ϕ/ϕ_y	0.303	0.543	0.860	1.000	1.620	3.880	10.900	∞
ϵ_s	0.000321	0.000622	0.000874	0.00102	($\epsilon_s = \epsilon_y$ Steel Starts To Yield)			

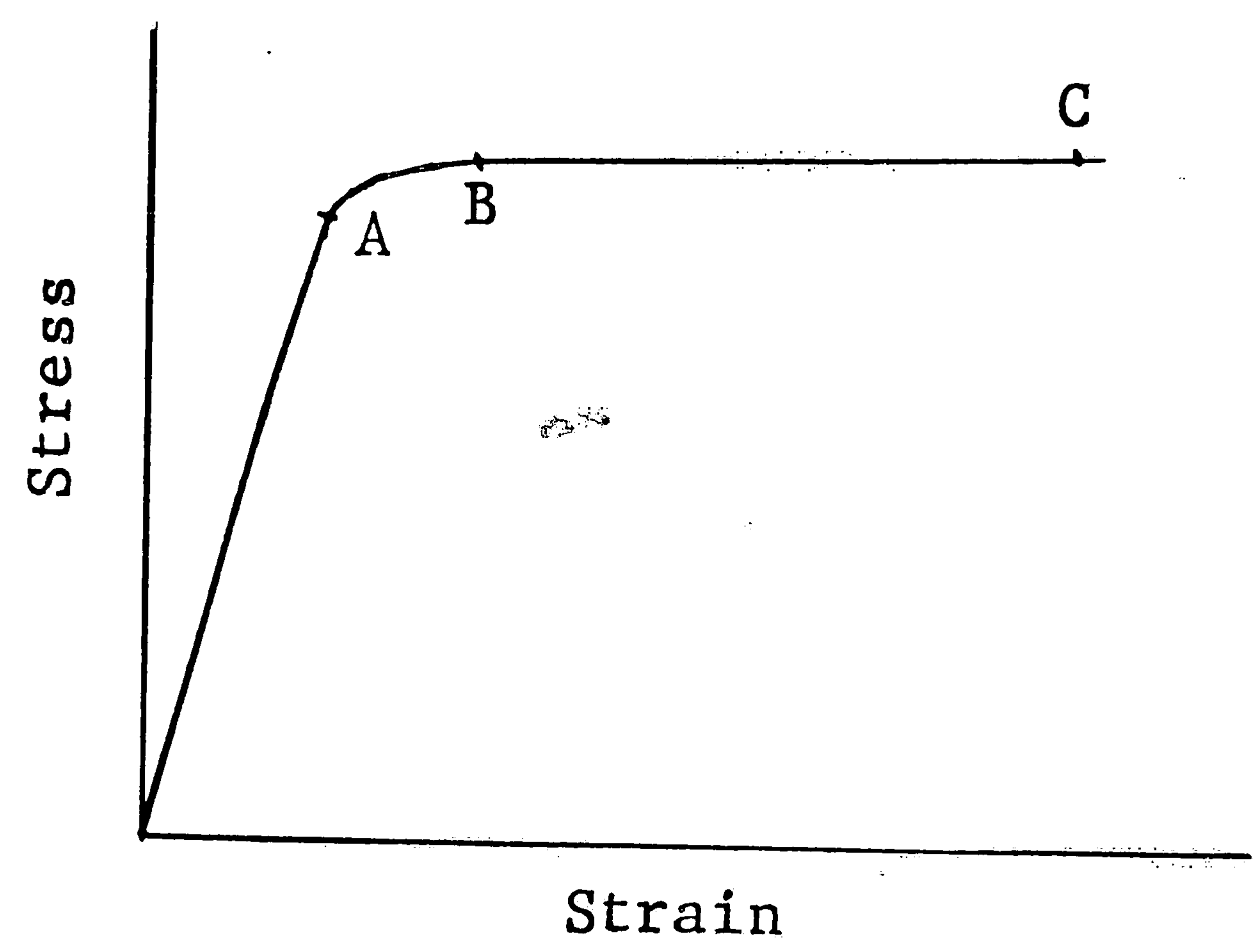

Fig. 1 STRESS-STRAIN RELATIONSHIP IN STEEL

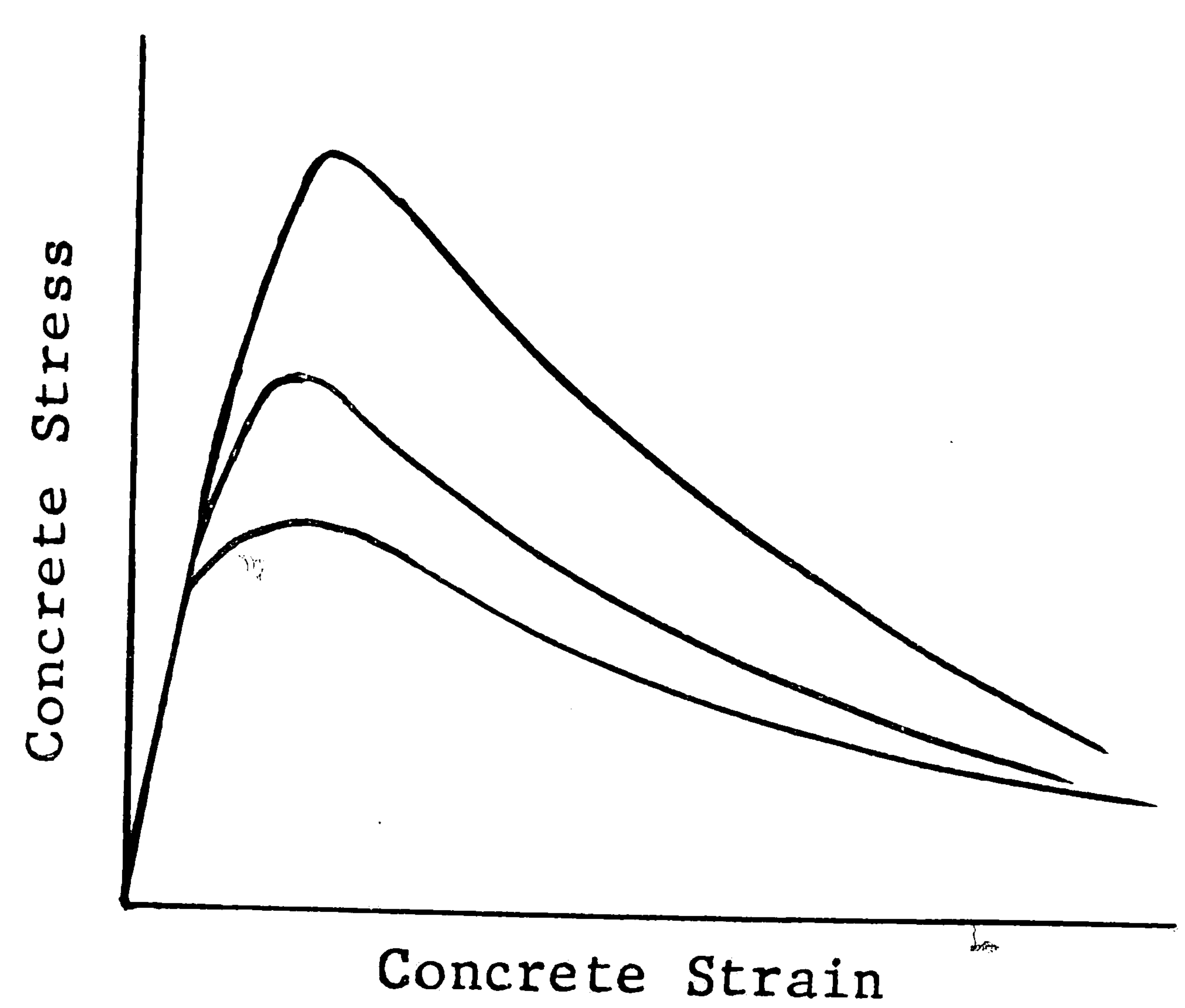

Fig. 2 CONCRETE STRESS-STRAIN CURVES BEYOND MAXIMUM STRESS (OBSERVED BY THE U.S. BUREAU OF RECLAMATION)

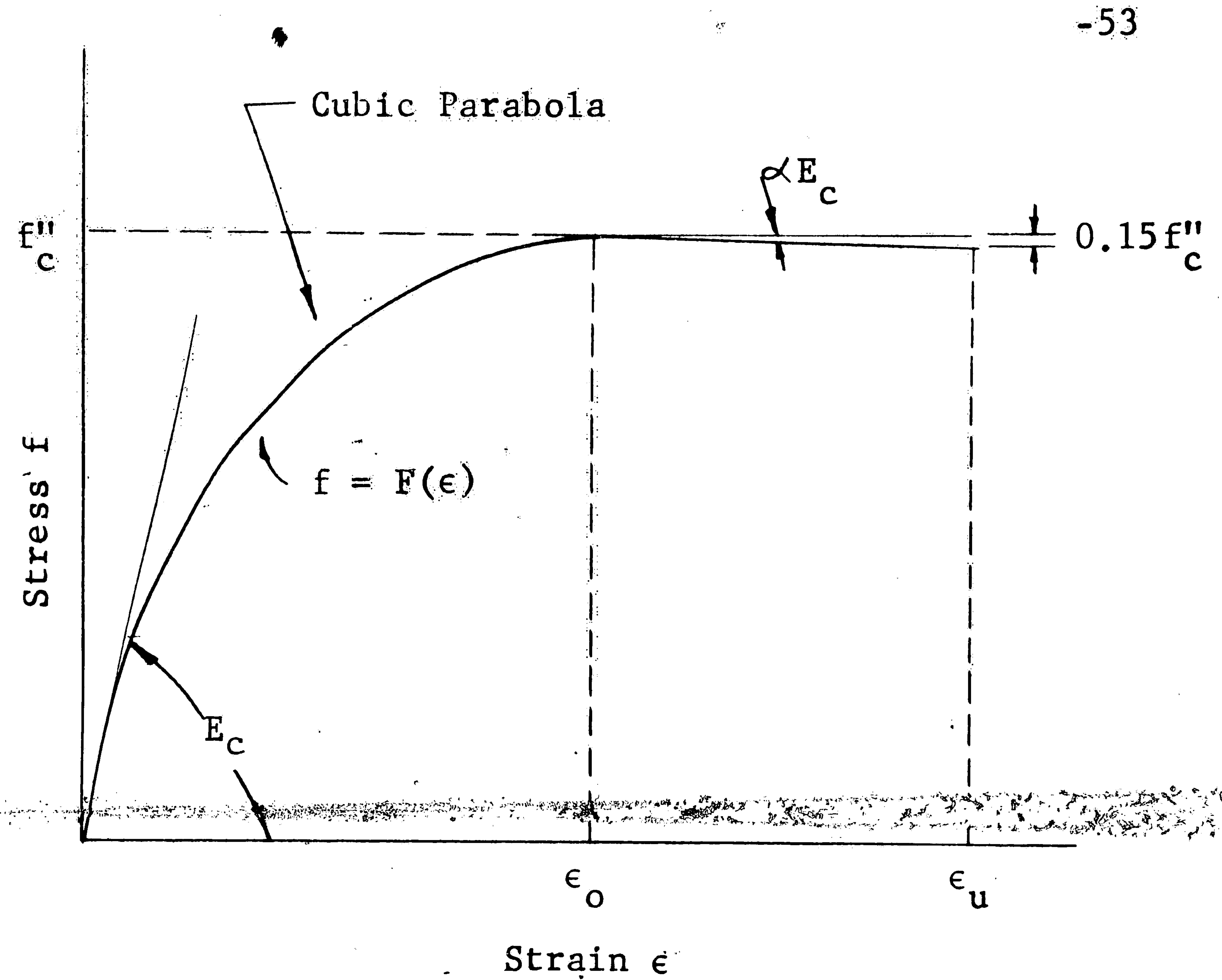

Fig. 3 GENERALIZED STRESS-STRAIN RELATIONSHIP FOR BOTH BOUND AND PLAIN CONCRETE

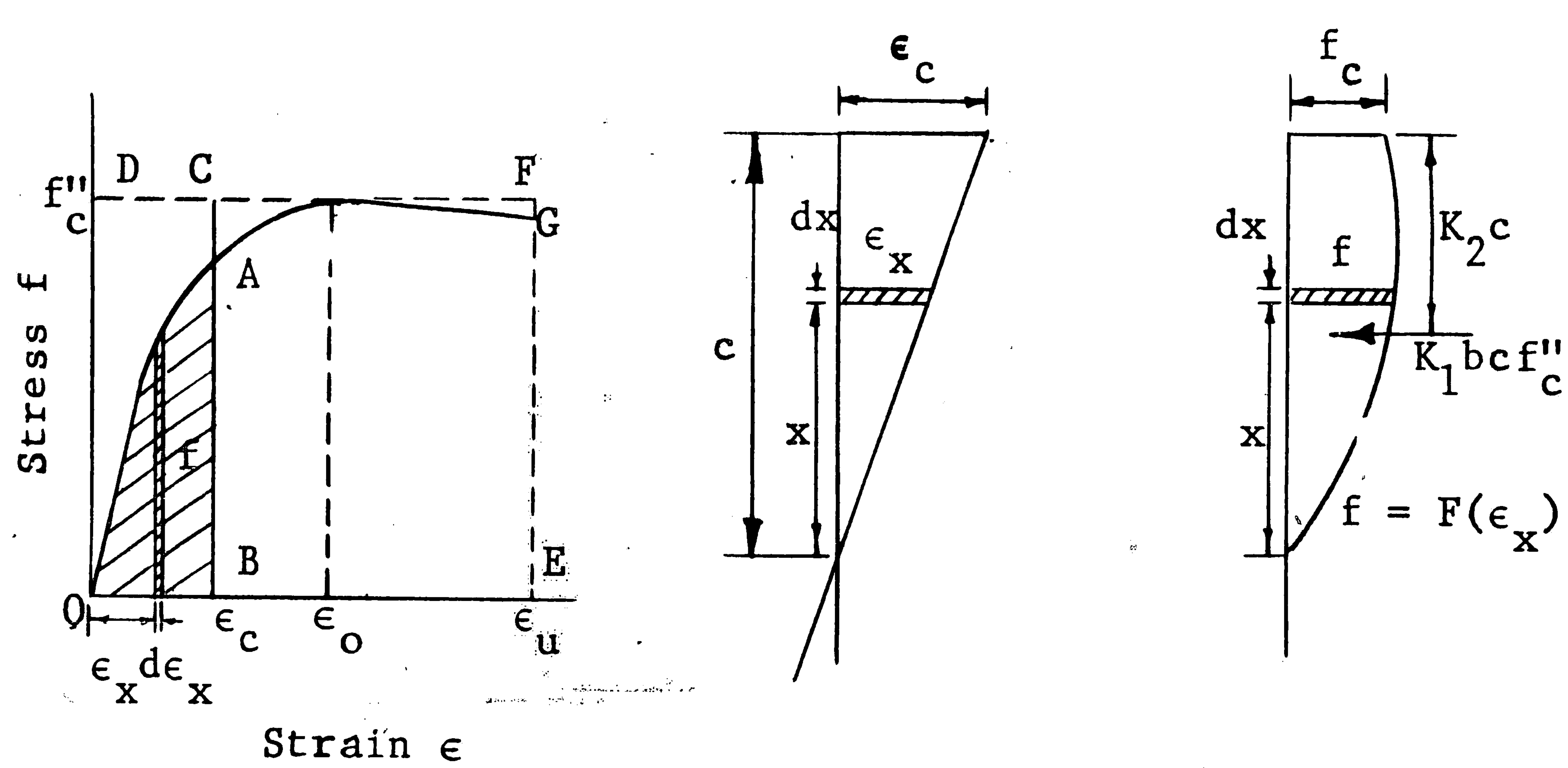

(a) Stress-Strain Relation (b) Strain (c) Stress

Fig. 4 DERIVATION OF CONCRETE COMPRESSIVE STRESS FACTOR K_1 AND K_2 AT ANY STRESS STAGE (See Chapter 2, section 2.3)

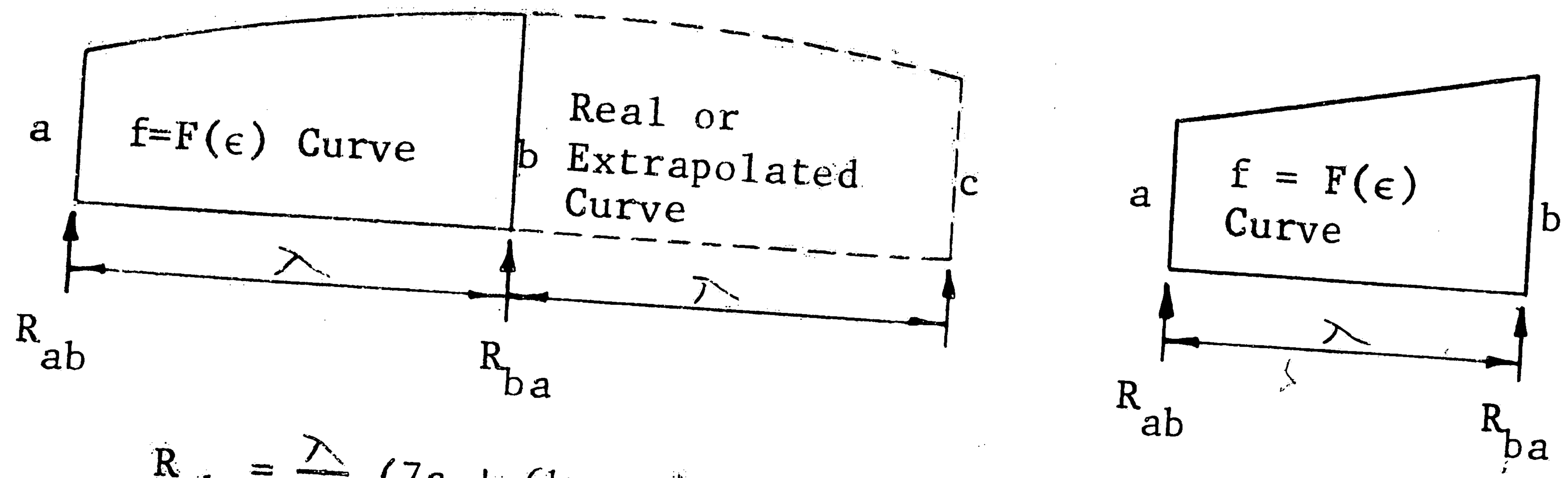

$$R_{ab} = \frac{\lambda}{24}(7a + 6b - c)$$

$$R_{ba} = \frac{\lambda}{24}(3a + 10b - c)$$

(a) For Smooth Curve

$$R_{ab} = \frac{\lambda}{6}(2a + b)$$

$$R_{ba} = \frac{\lambda}{6}(a + 2b)$$

(b) For Polygonal Curve

Fig. 5 FORMULAS FOR EQUIVALENT CONCENTRATED LOADS

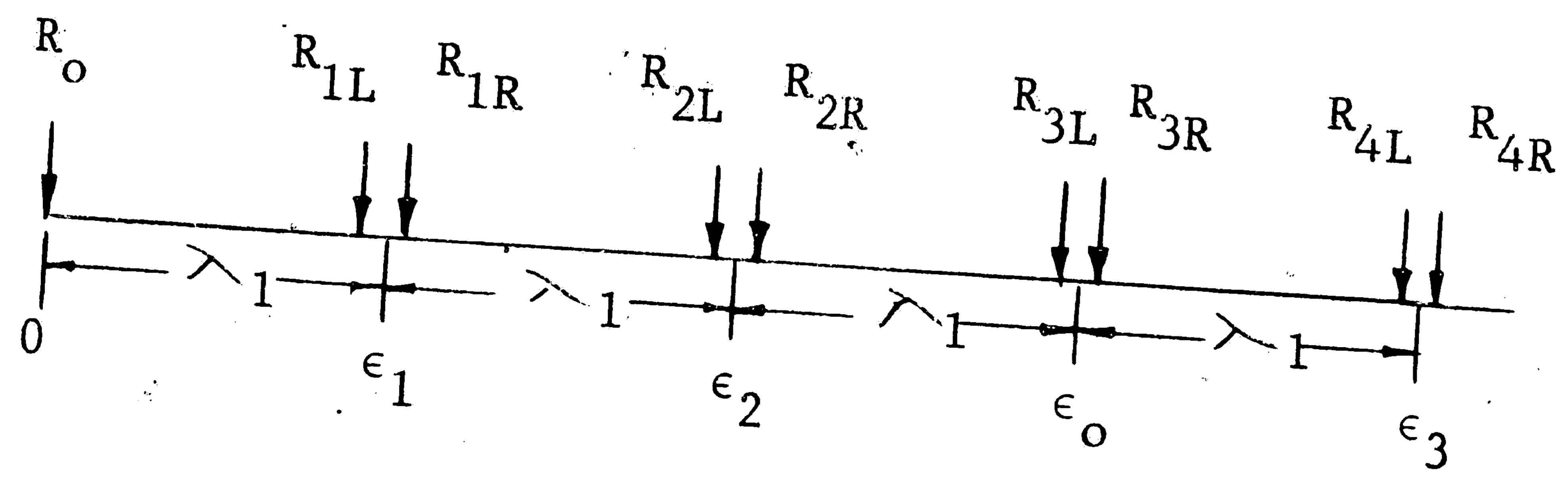

Fig. 6 A SERIES OF CONCENTRATED REACTIONS
(See Chapter 2, section 2.4.2)

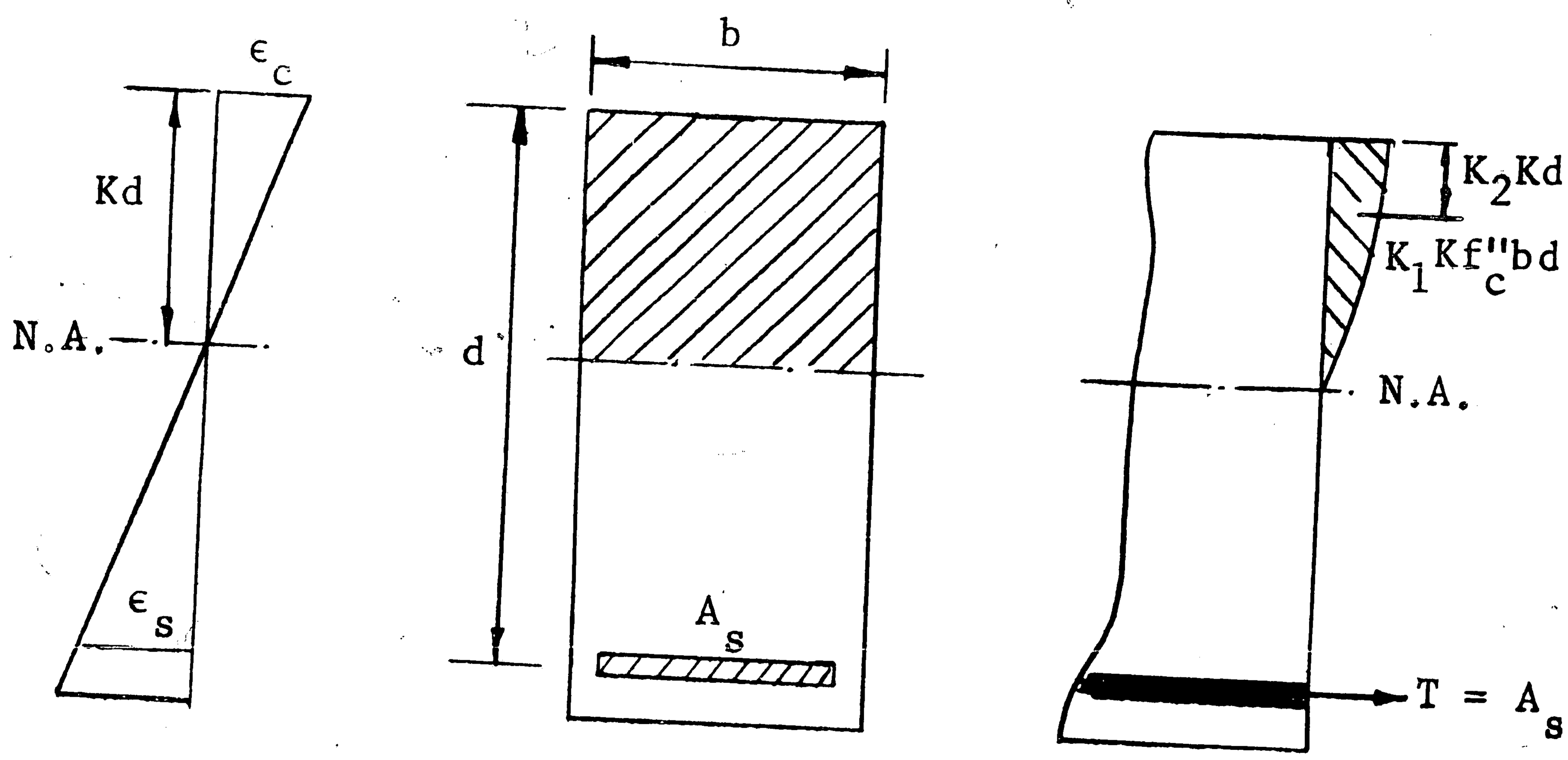

(a) Strain Distribution (b) Section (c) Stress Distribution

Fig. 7 RECTANGULAR BEAM WITH TENSION REINFORCEMENT ONLY
(See Chapter 2, section 2.5.1)

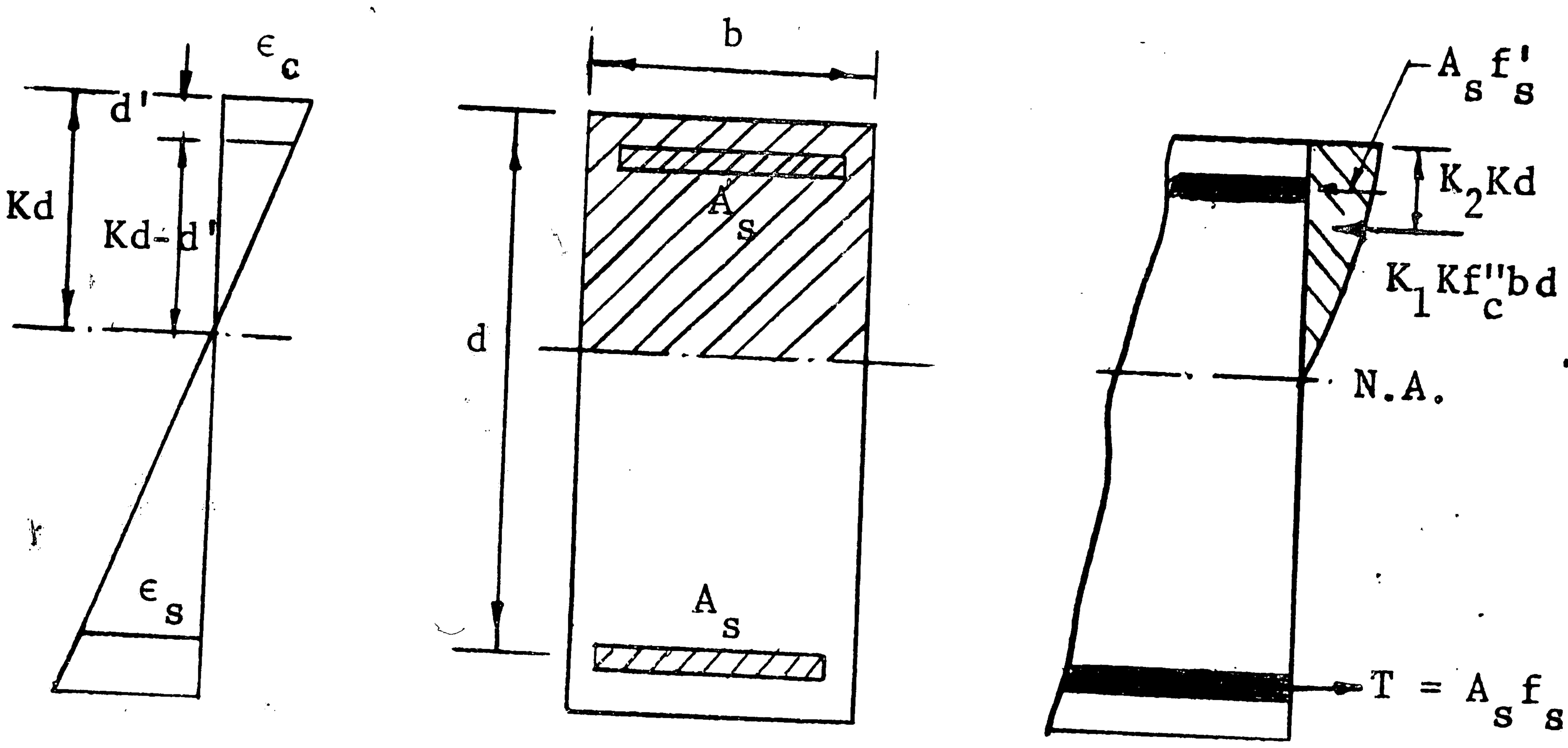

(a) Strain Distribution (b) Section (c) Stress Distribution

Fig. 8 RECTANGULAR BEAM WITH COMPRESSION REINFORCEMENTS
(See Chapter 2, section 2.5.2)

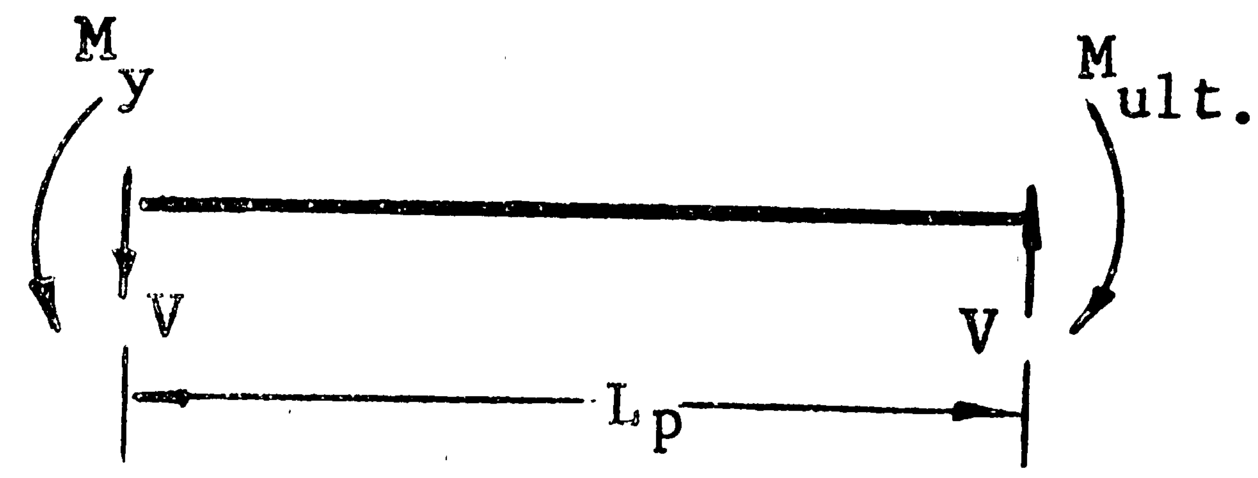

Fig. 9 PLASTIC LENGTH L_p
(See Chapter 2, section 2.6)

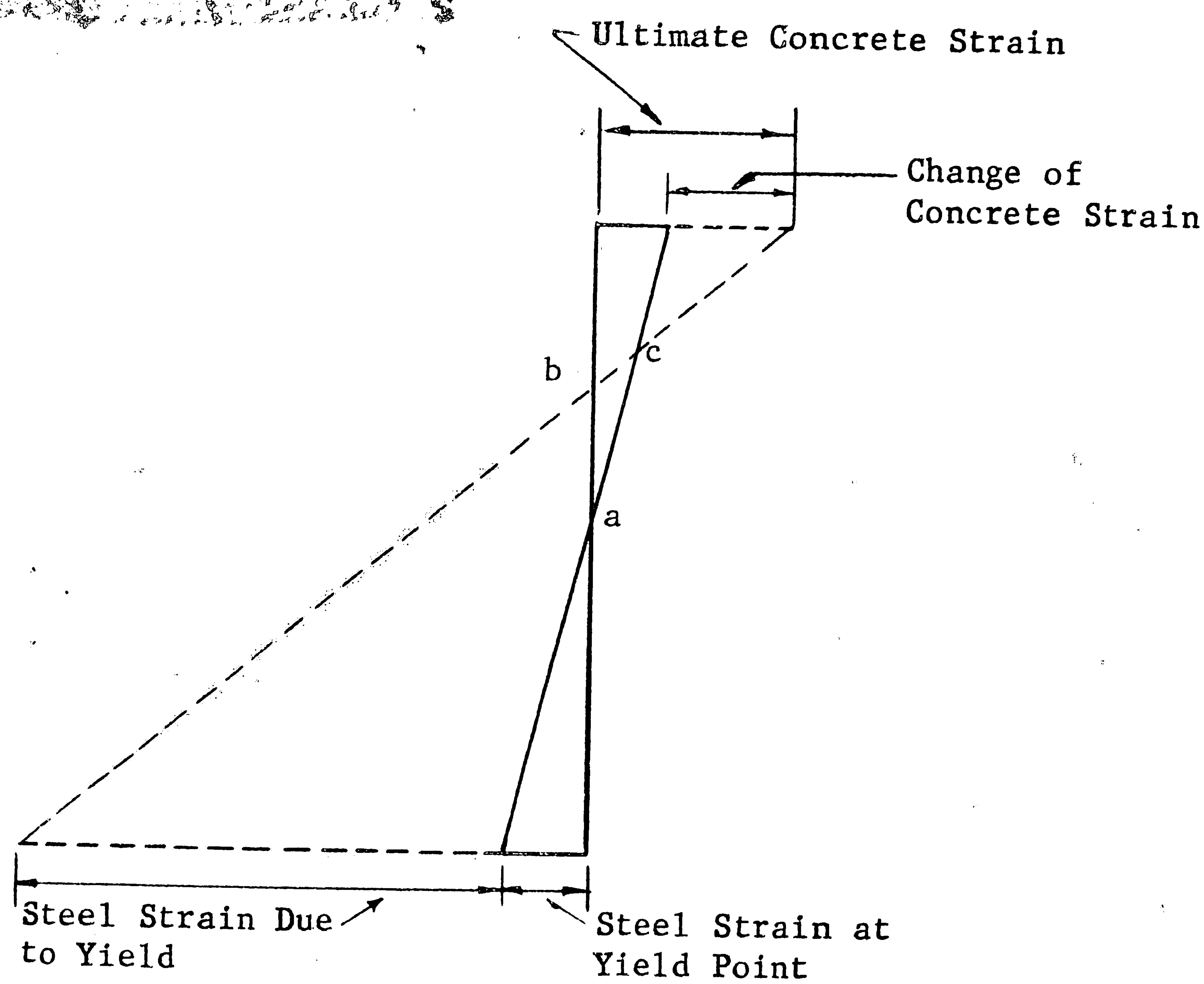

Fig. 10 TENSILE PLASTIC HINGES
(See Chapter 2, section 2.7.1)

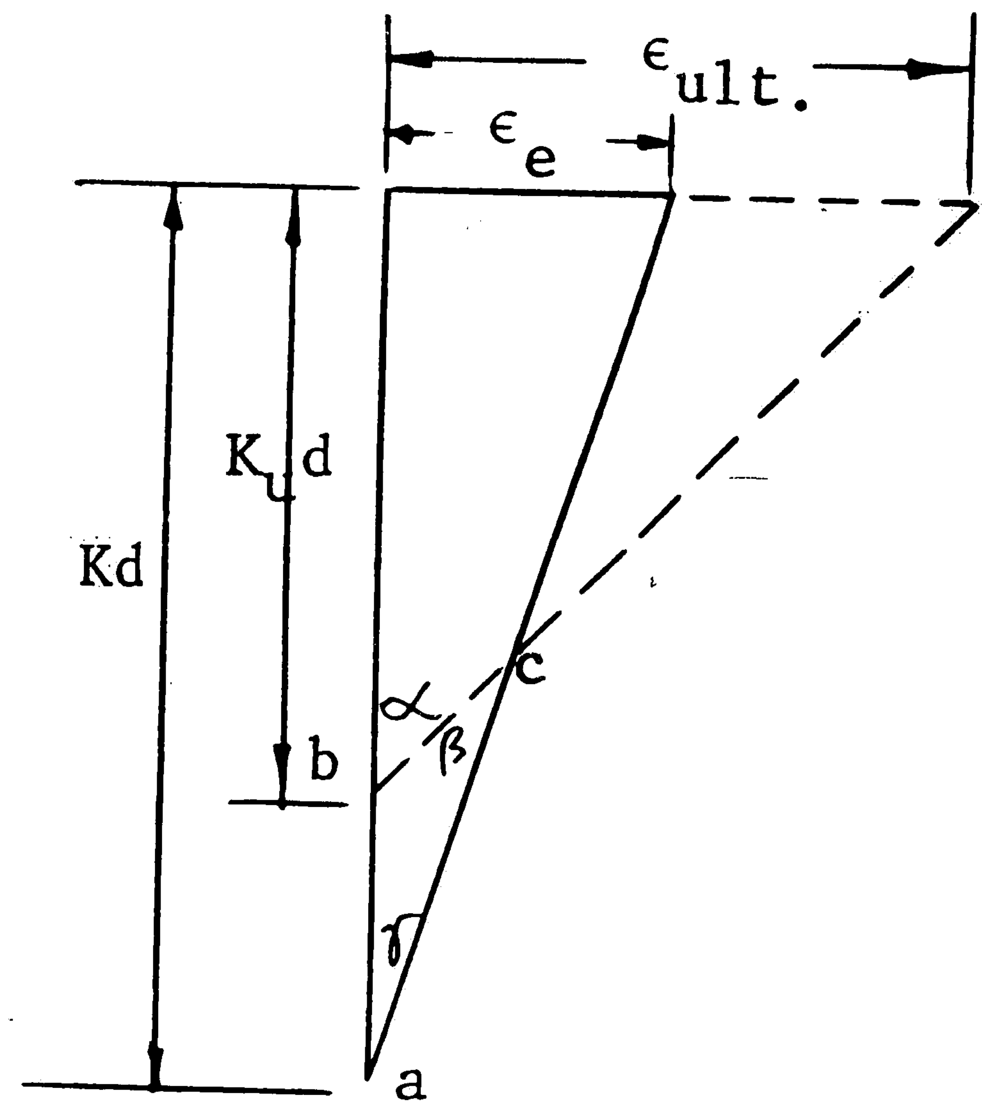

Fig. 11 ELASTIC ROTATION AND PLASTIC ROTATION
(See Chapter 2, section 2.7.1)

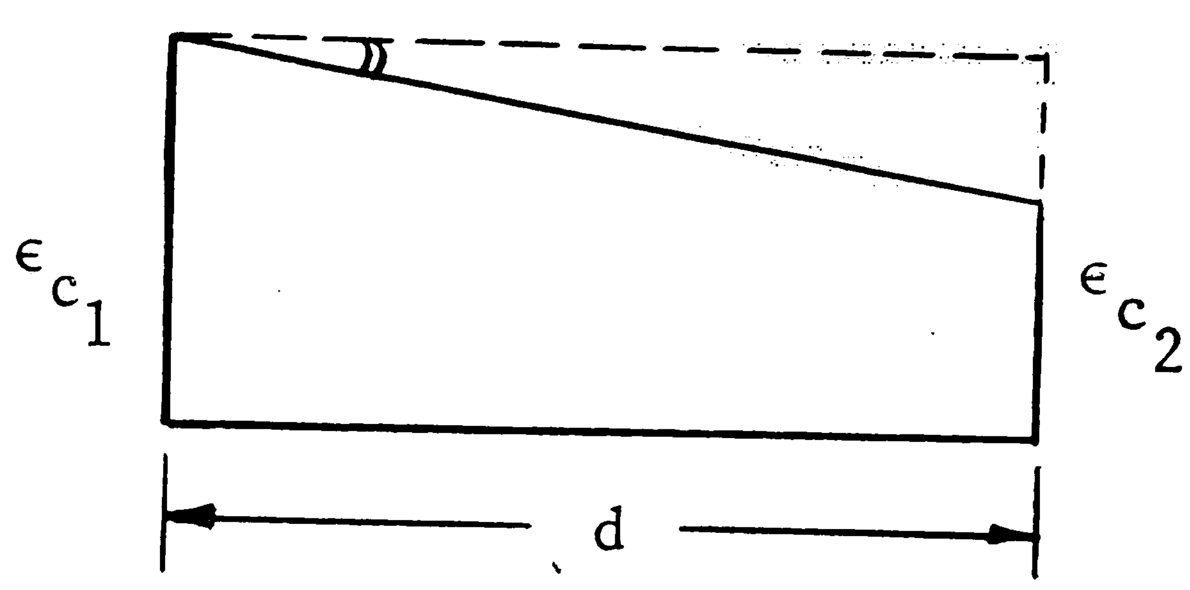

Fig. 12 COMPRESSIVE HINGES
(See Chapter 2, section 2.7.2)

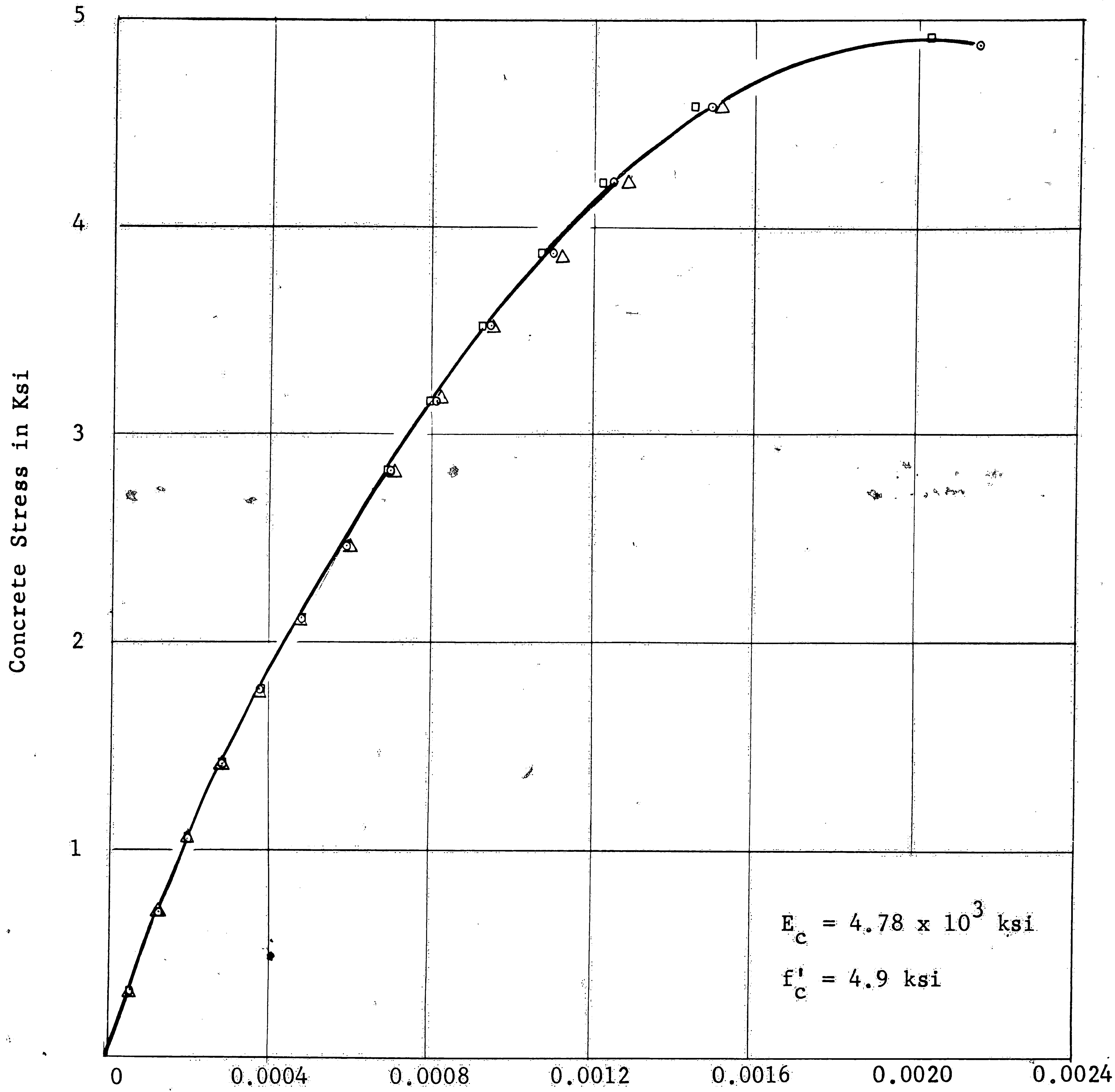

Fig. 13a STRESS-STRAIN RELATIONSHIP FOR THREE 6 x 12 IN. CYLINDERS AT 28 DAYS

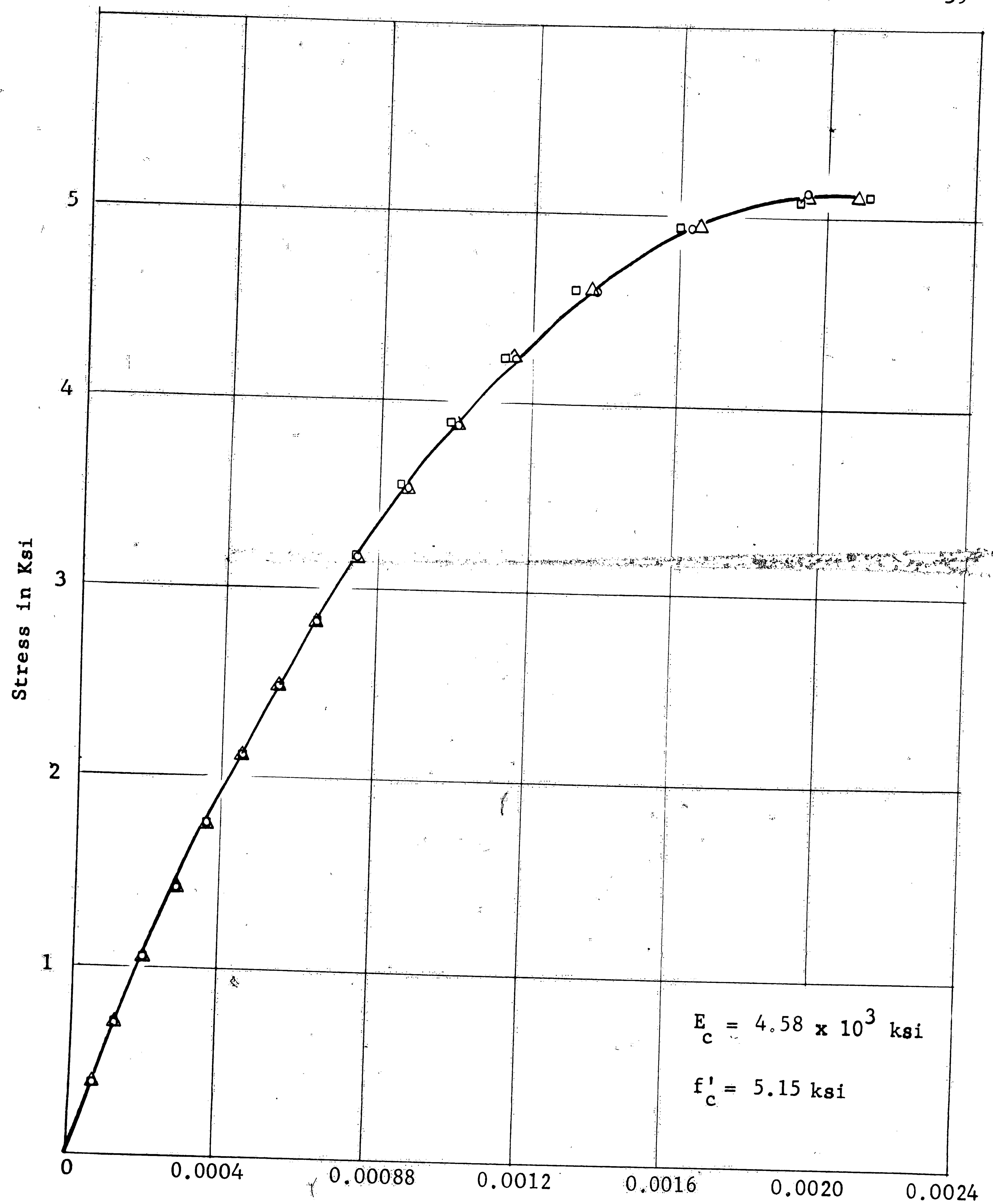

Fig. 13b STRESS-STRAIN RELATIONSHIP FOR THREE 6 x 12 IN. CYLINDERS AT 35 DAYS

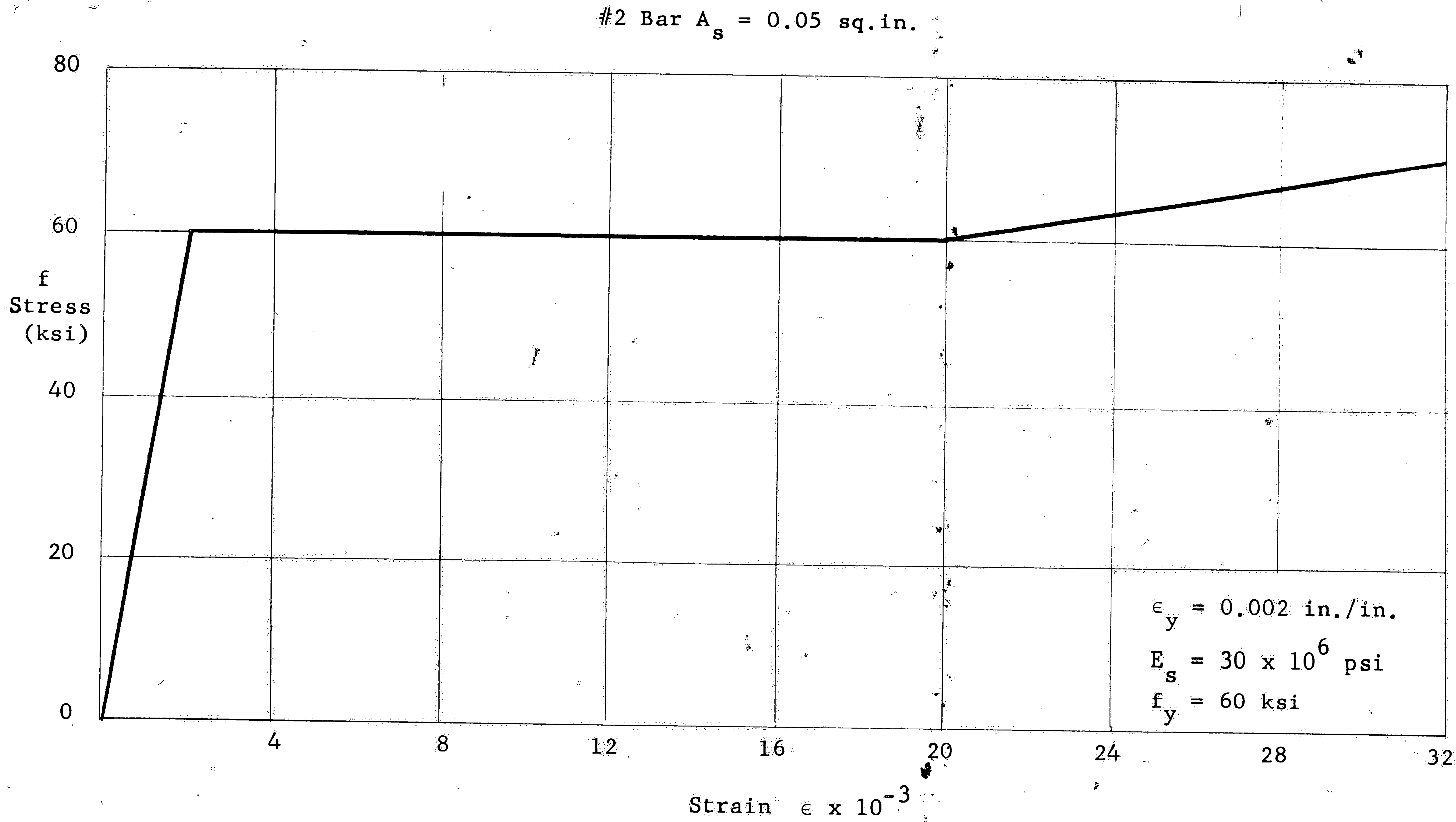

Fig. 14 IDEALIZED STRESS-STRAIN CURVE FOR NO. 2 DEFORMED BARS

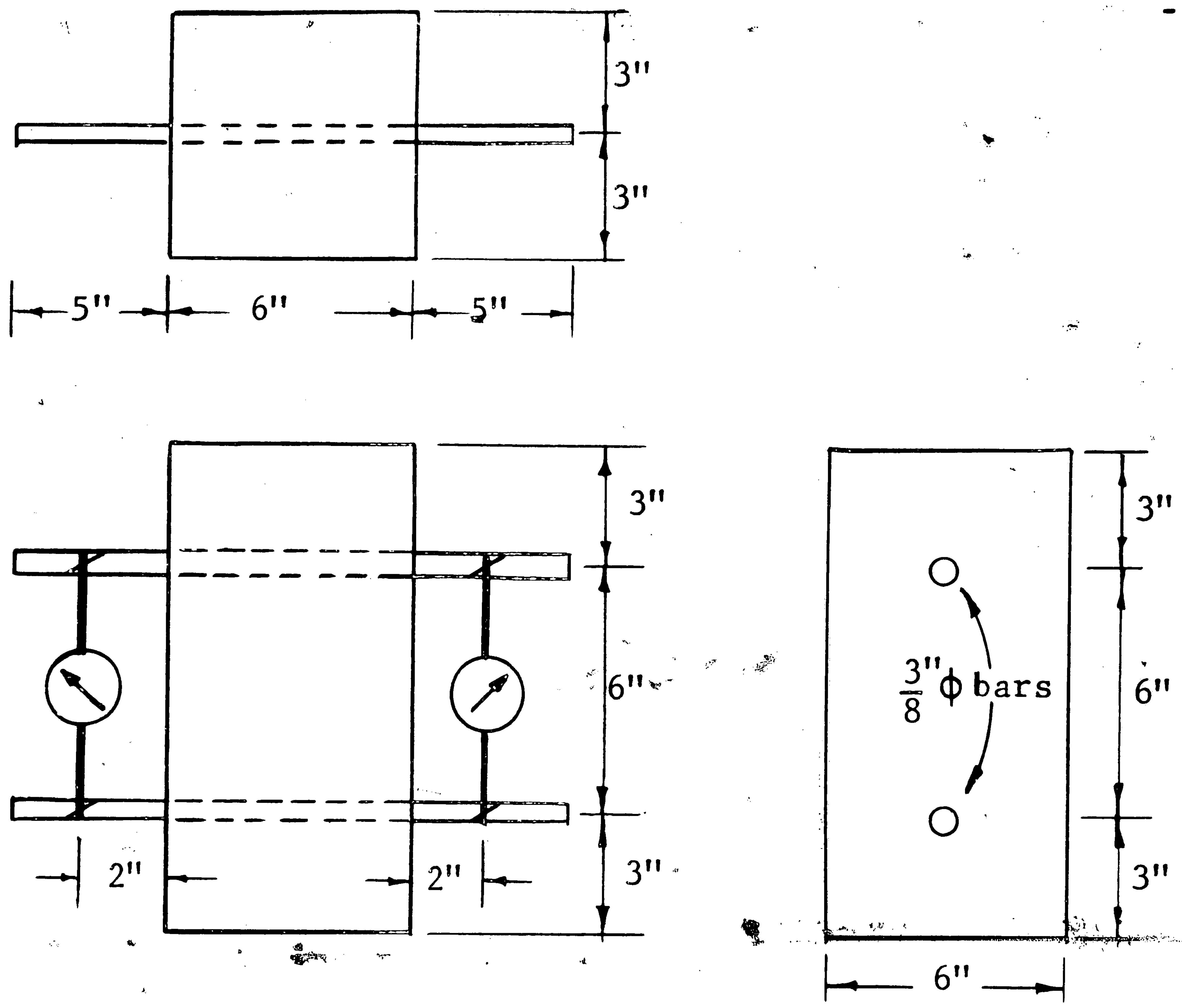

Fig. 15 DETAILS OF THE TEST SPECIMENS No. 1, No. 2, No. 3

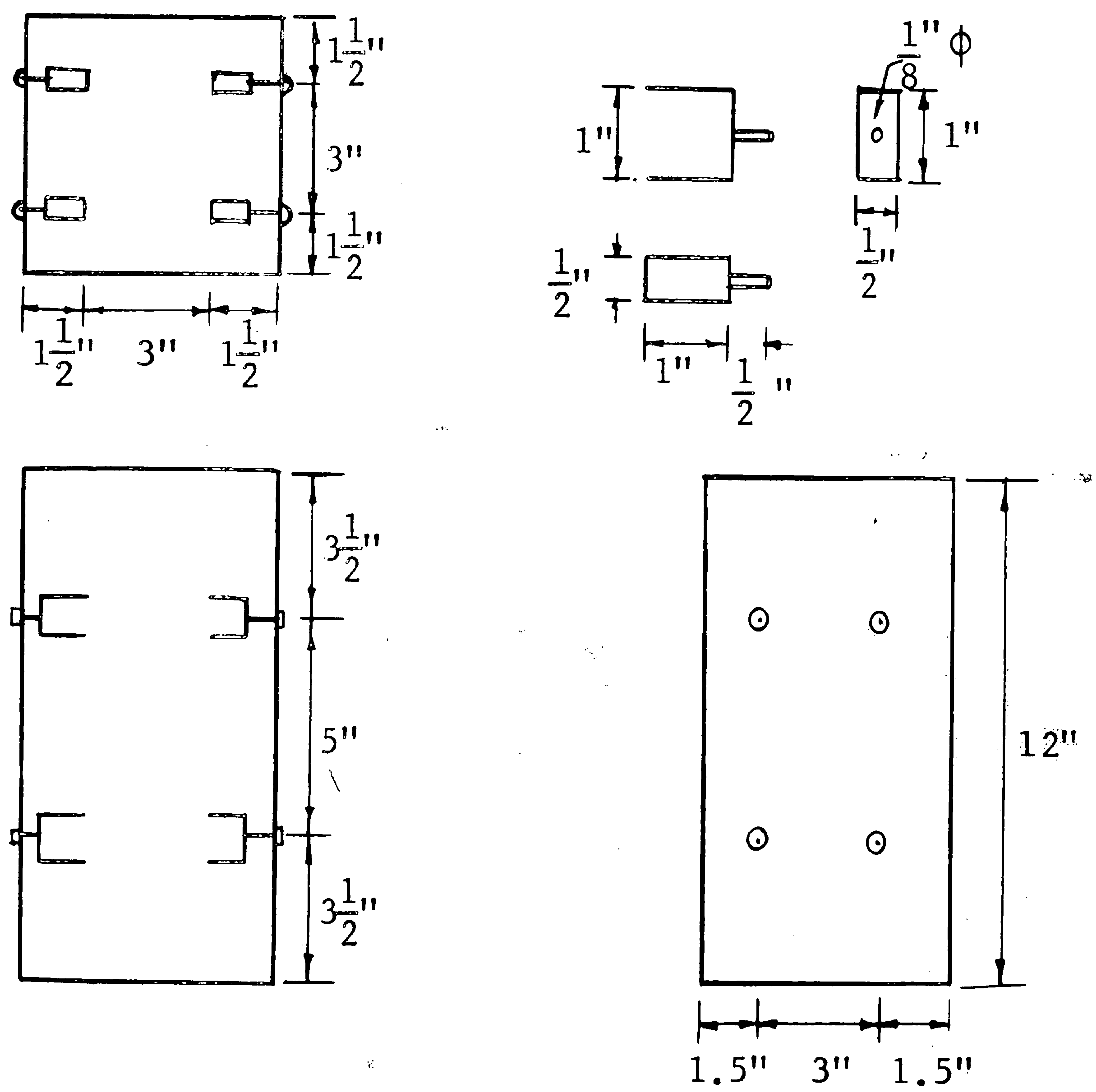

Fig. 16 DETAILS OF THE TEST SPECIMENS No. 4, No. 5, No. 6

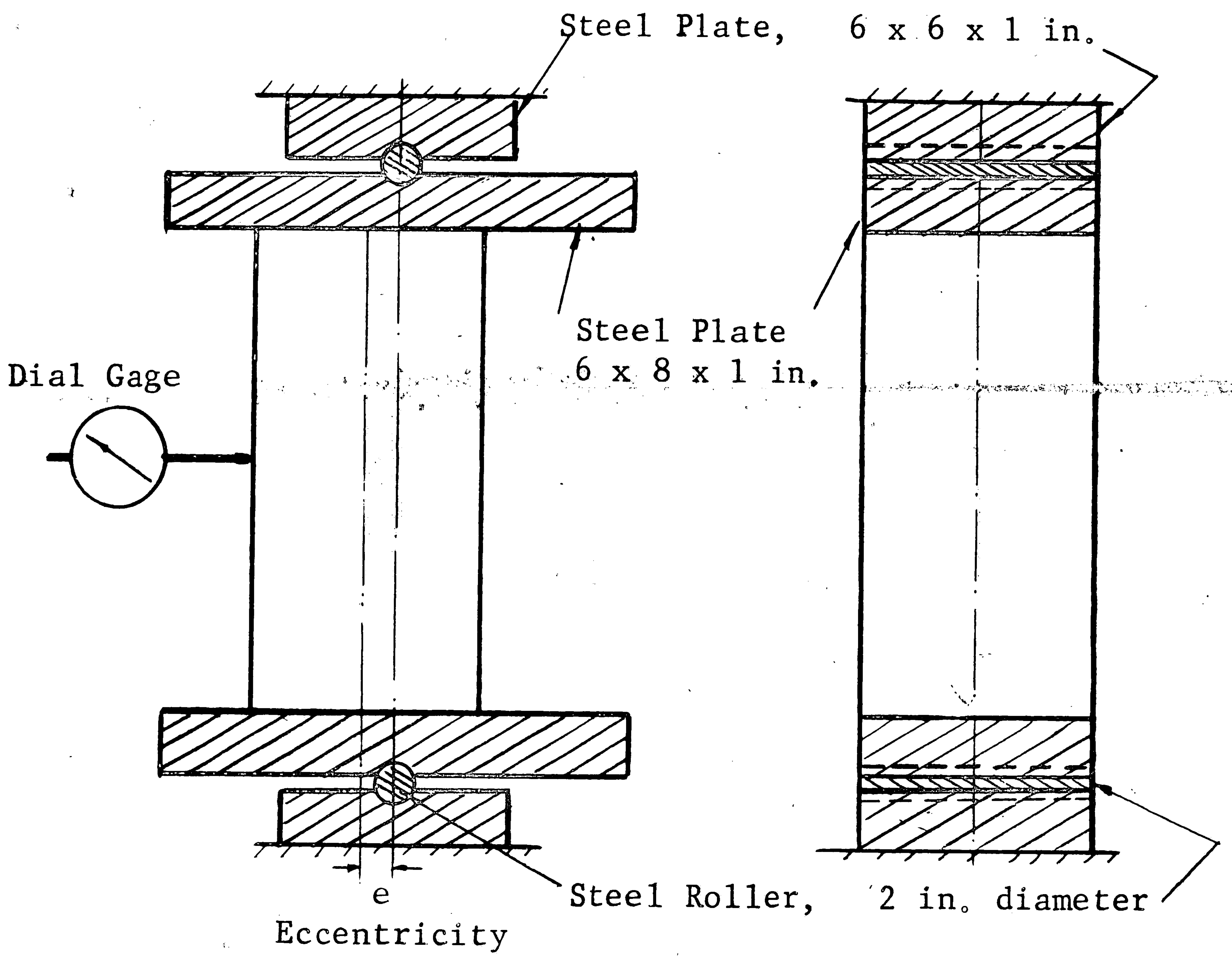

Fig. 17 LOADING ARRANGEMENT

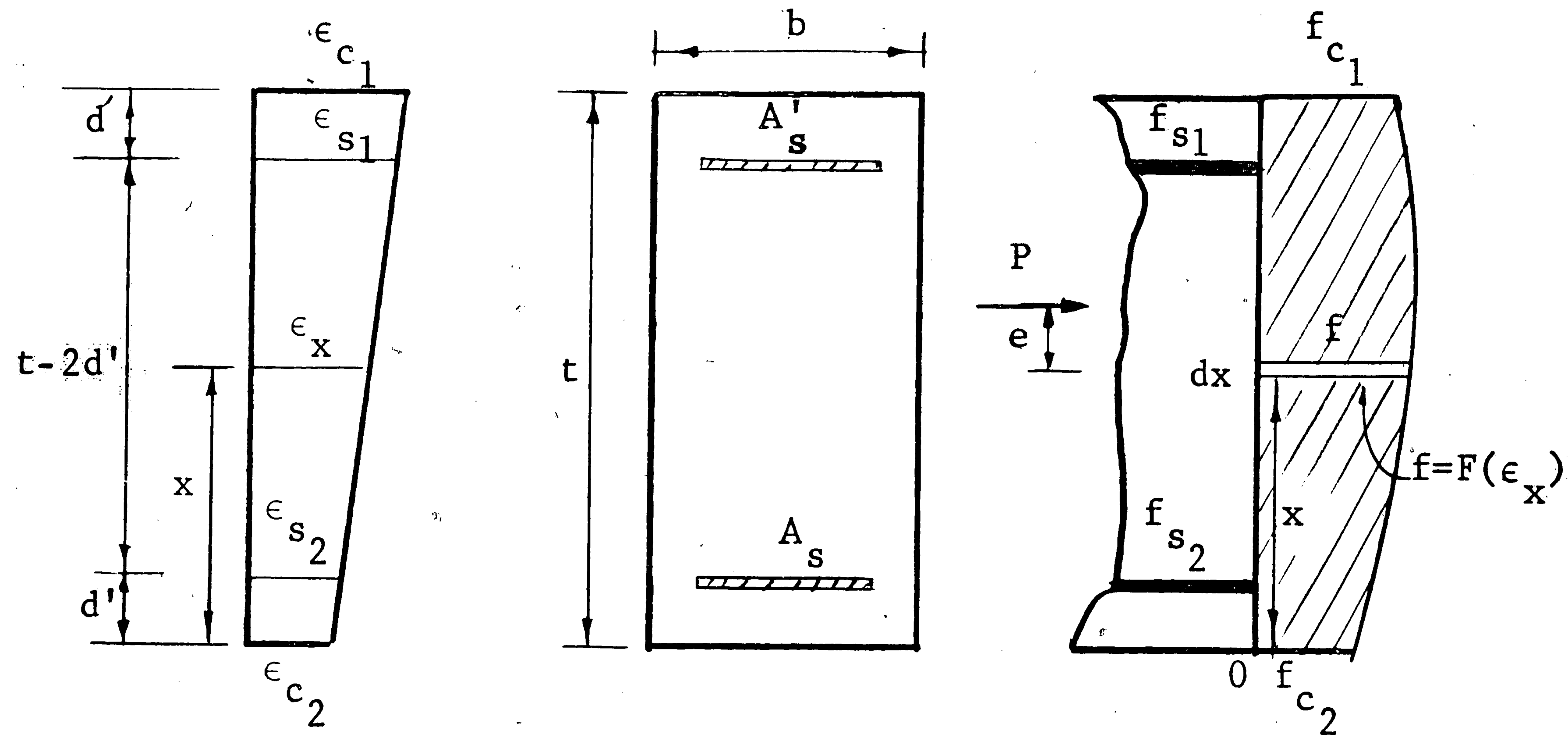

(a) Strain Distribution (b) Section (c) Stress Distribution

Fig. 18 STRESS ANALYSIS,(N.A. OUTSIDE THE SECTION)
(See Chapter 3, section 3.4.1)

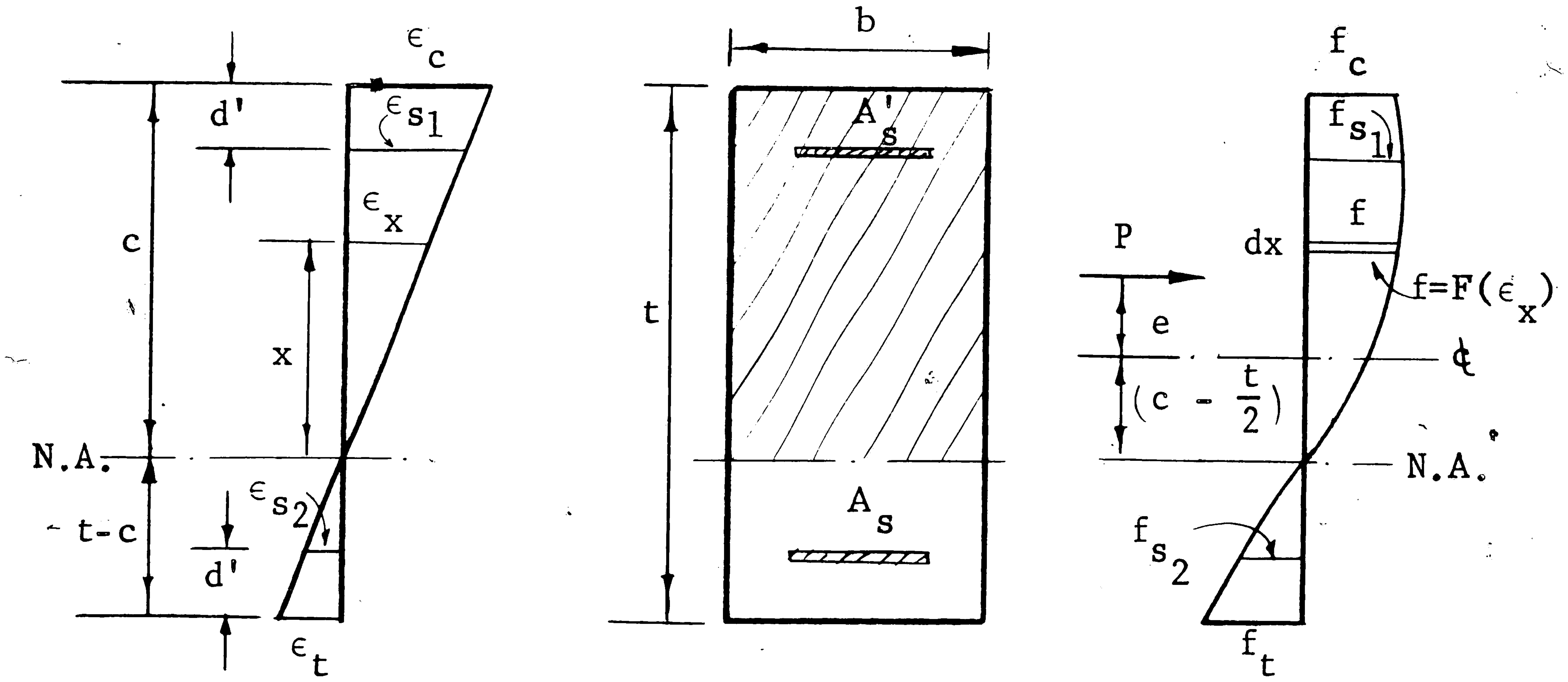

(a) Strain Distribution (b) Section (c) Stress Distribution

Fig. 19 STRESS ANALYSIS,(N.A. INSIDE THE SECTION)
(See Chapter 3, section 3.4.2)

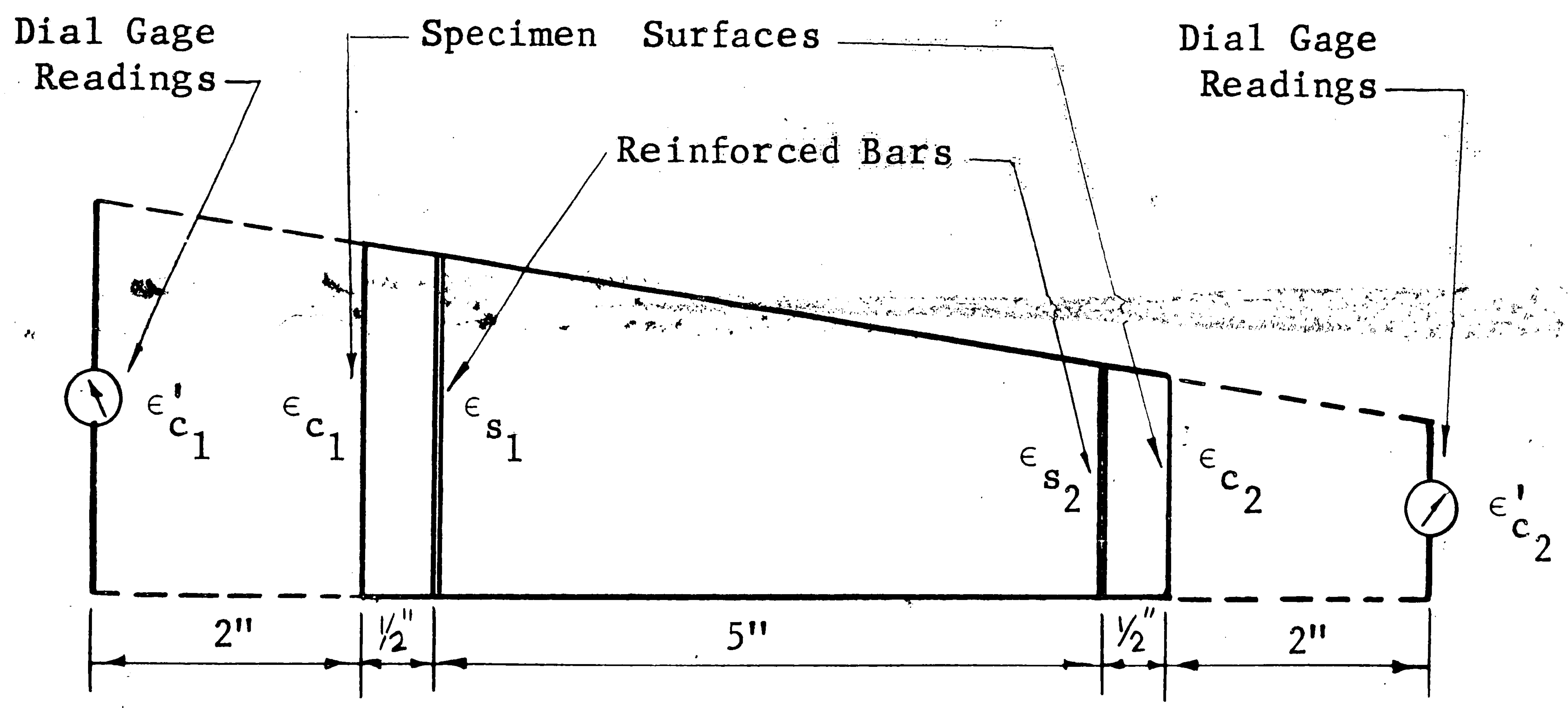

Fig. 20 STRAIN RELATIONSHIP OF TESTED SPECIMENS (See Chapter 3, section 3.5.1)

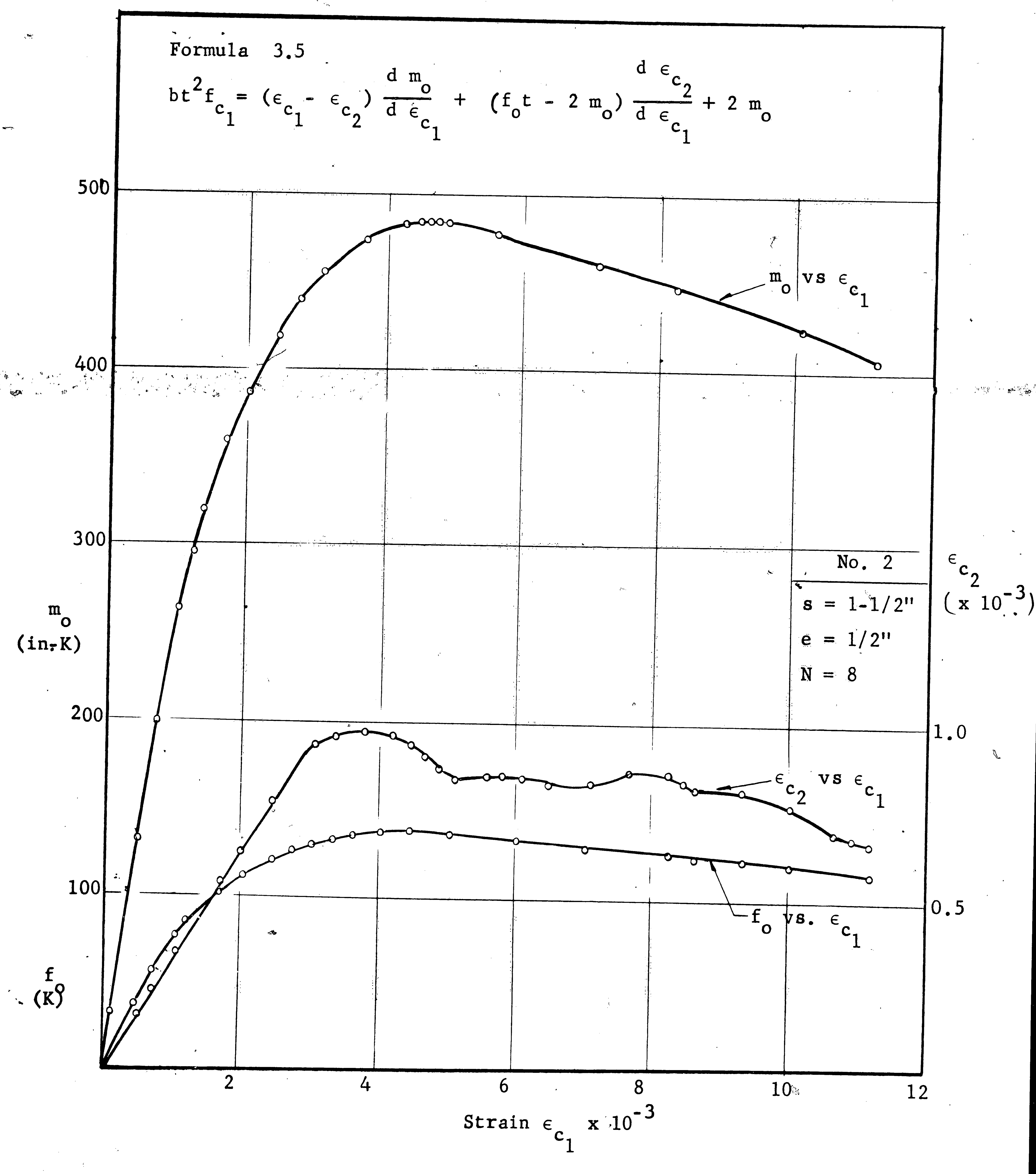

Fig. 21a m_o vs. ϵ_{c_1}, ϵ_{c_2} vs. ϵ_{c_1} and f_o vs ϵ_{c_1} CURVES

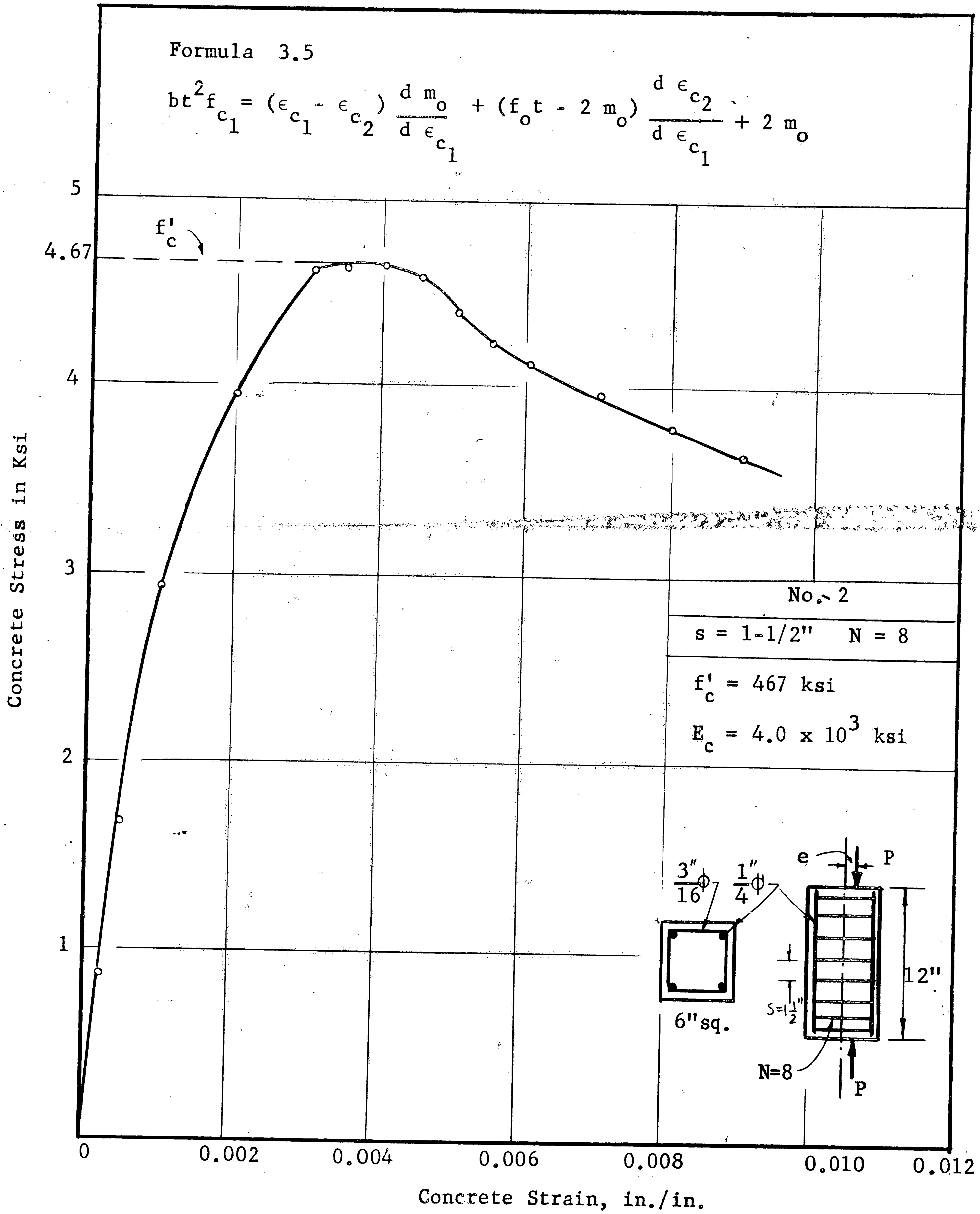

Fig. 21b STRESS-STRAIN RELATIONSHIP FOR BOUND CONCRETE, SPECIMEN NO. 2

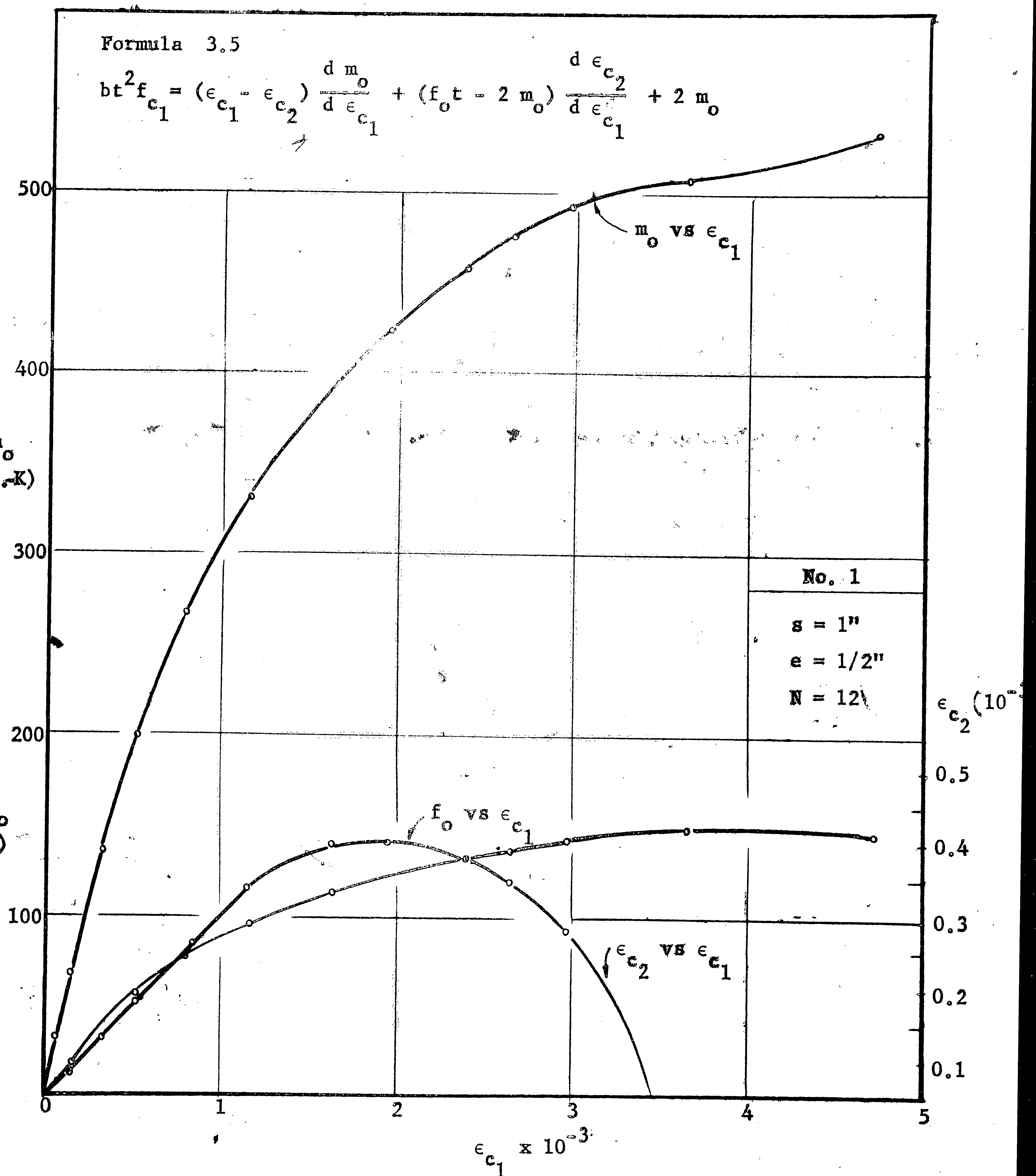

Fig. 22 m_o vs ϵ_{c_1}, ϵ_{c_2} vs ϵ_{c_1}, and f_o vs ϵ_{c_1} CURVES

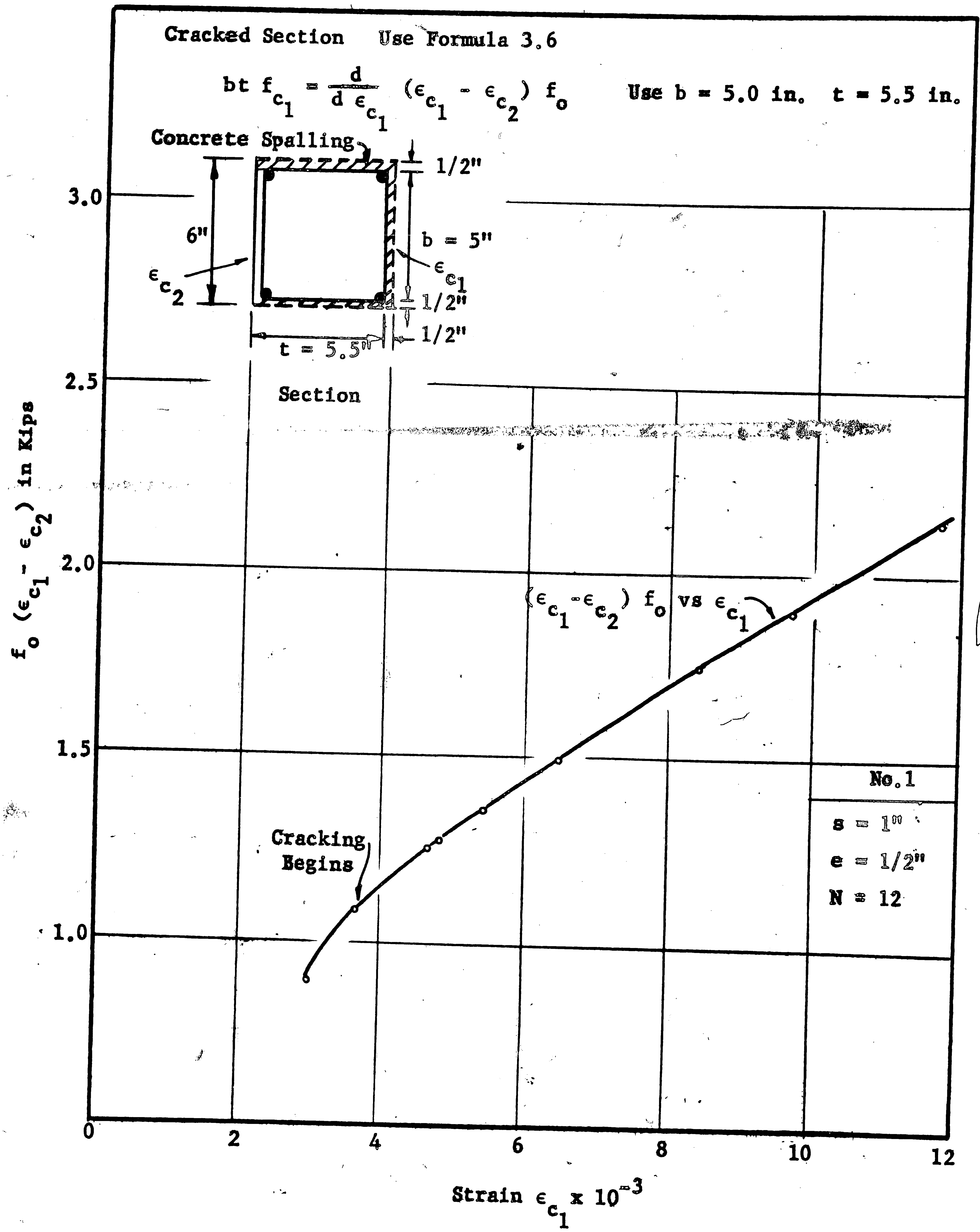

Fig. 22b $(\epsilon_{c_1} - \epsilon_{c_2})\, f_o$ vs ϵ_{c_1} CURVE

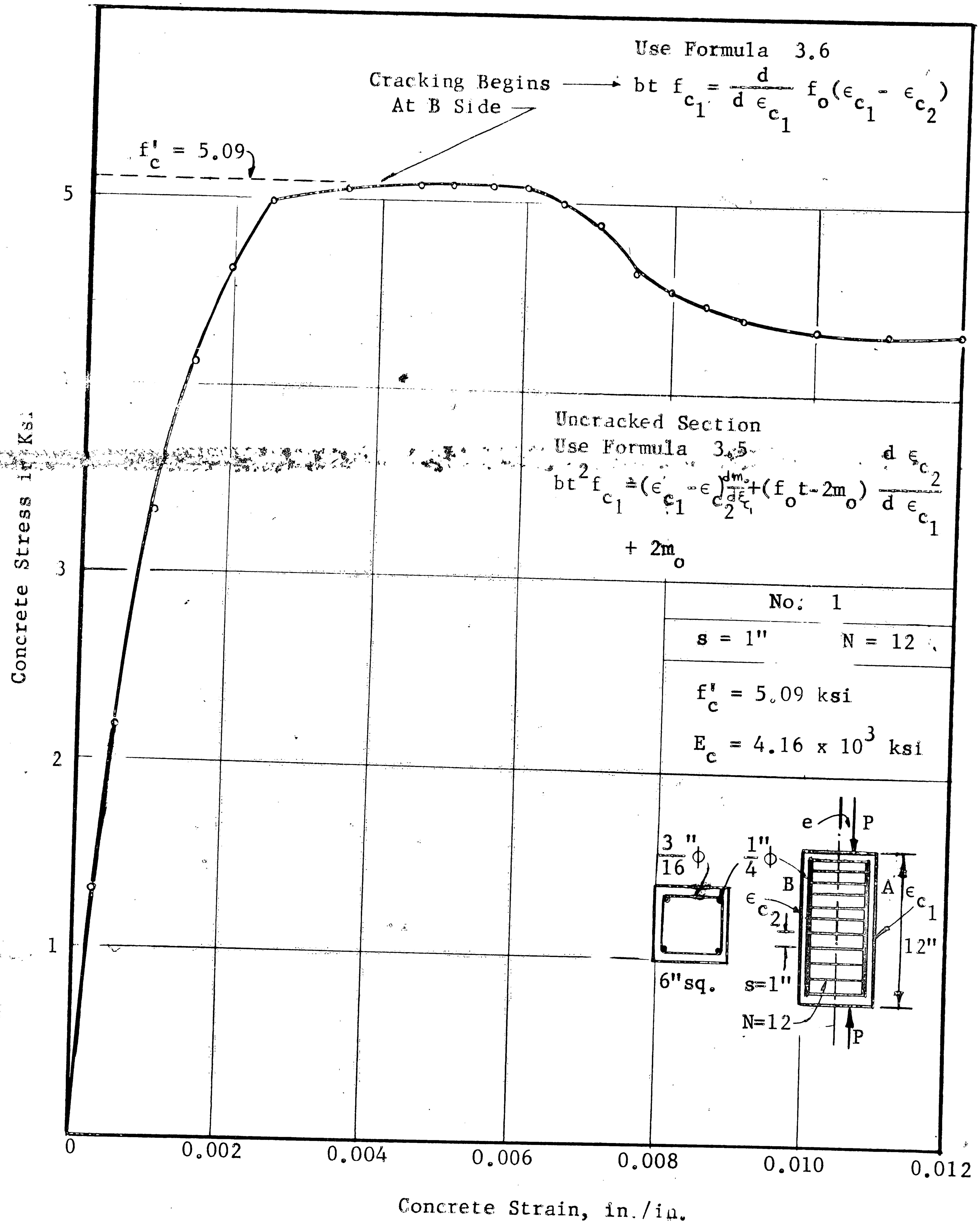

Fig. 22c STRESS-STRAIN RELATIONSHIP FOR BOUND CONCRETE

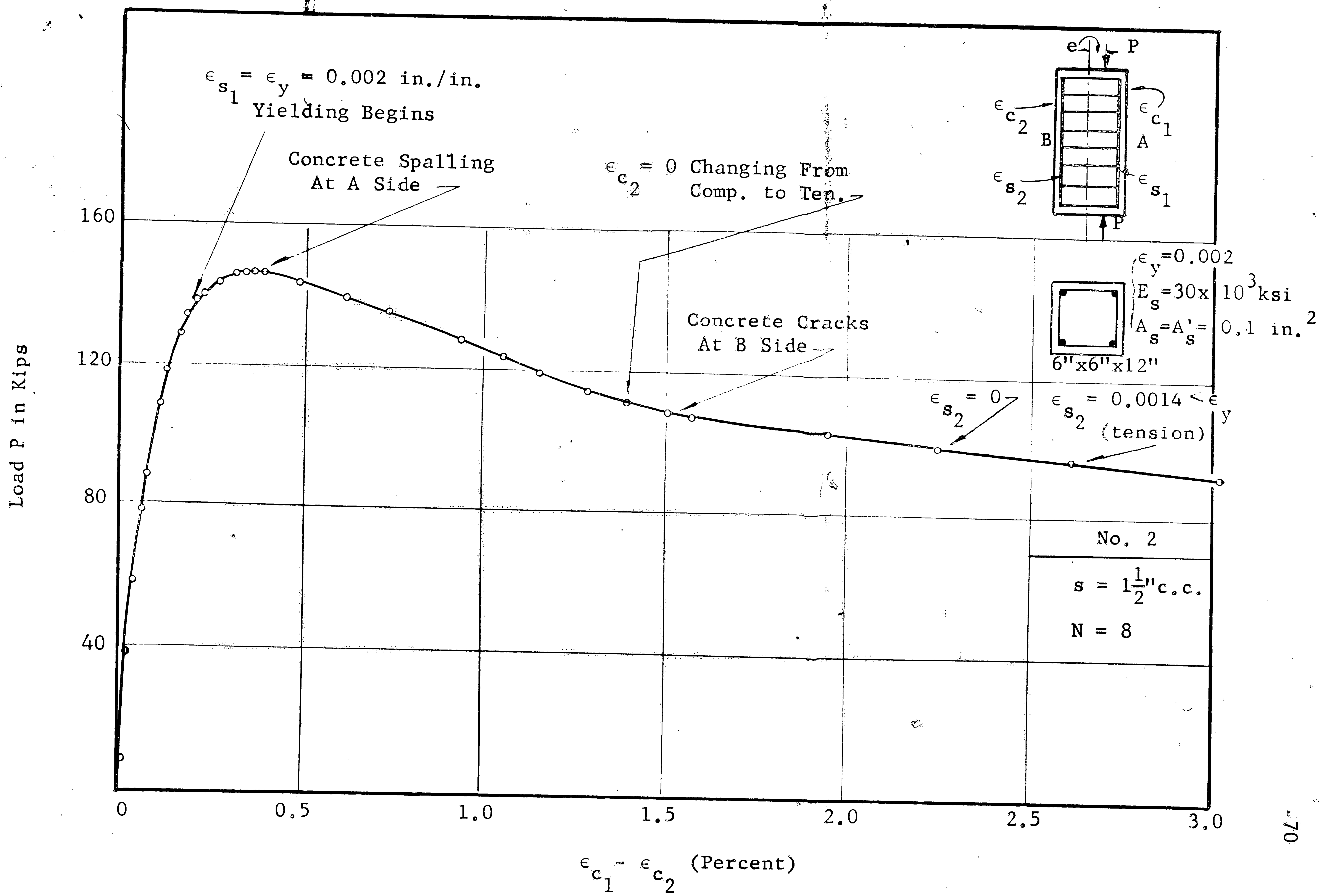

Fig. 23 LOAD VS STRAIN DIFFERENCE ACROSS SECTION (6"x 6"x 12" BOUNDED CONCRETE BLOCK)

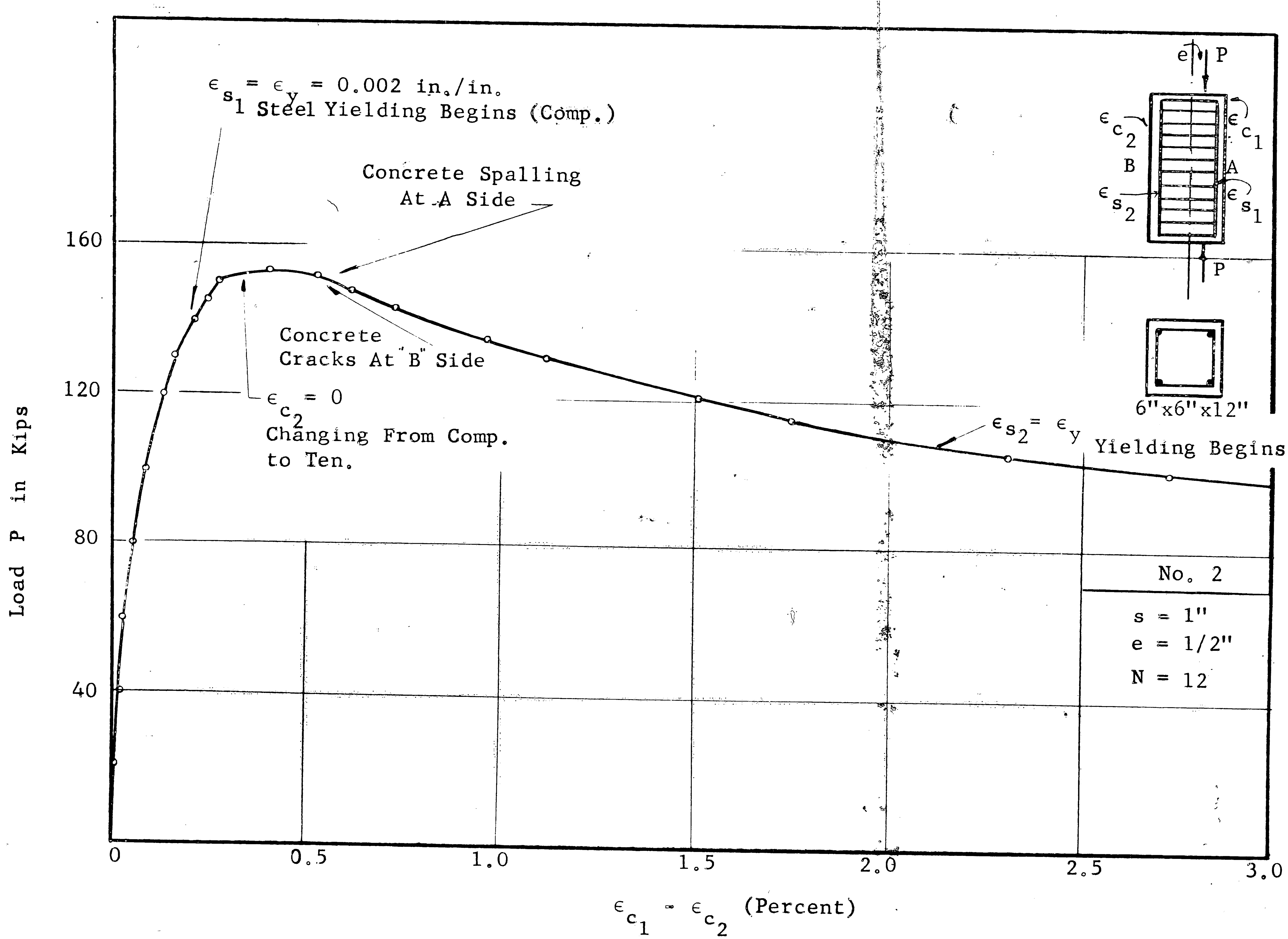

Fig. 24 LOAD VS STRAIN DIFFERENCE ACROSS SECTION
(6" x 6" x 12" BOUNDED CONCRETE BLOCK)

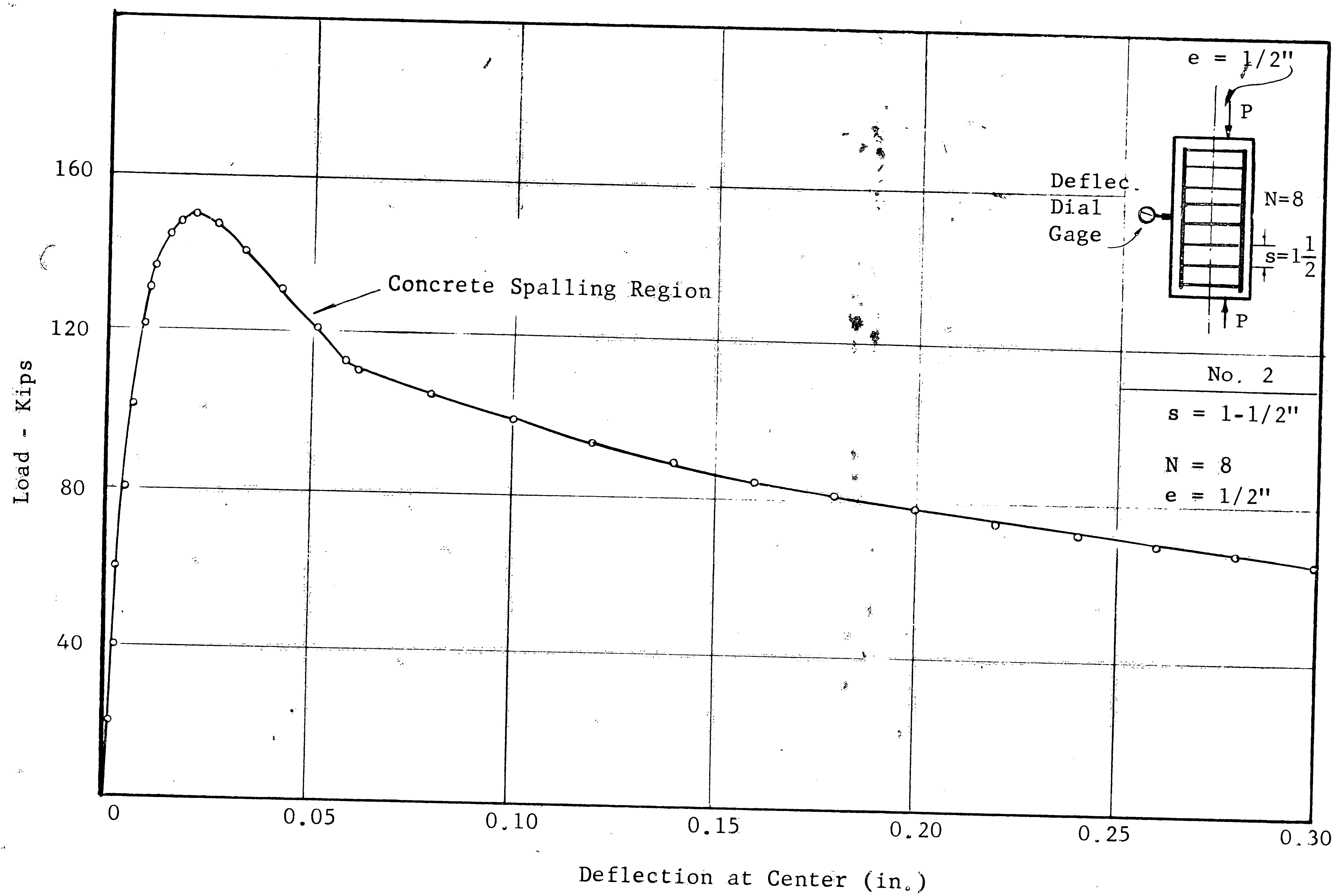

Fig. 25 TYPICAL DEFLECTION CURVE AT CENTER

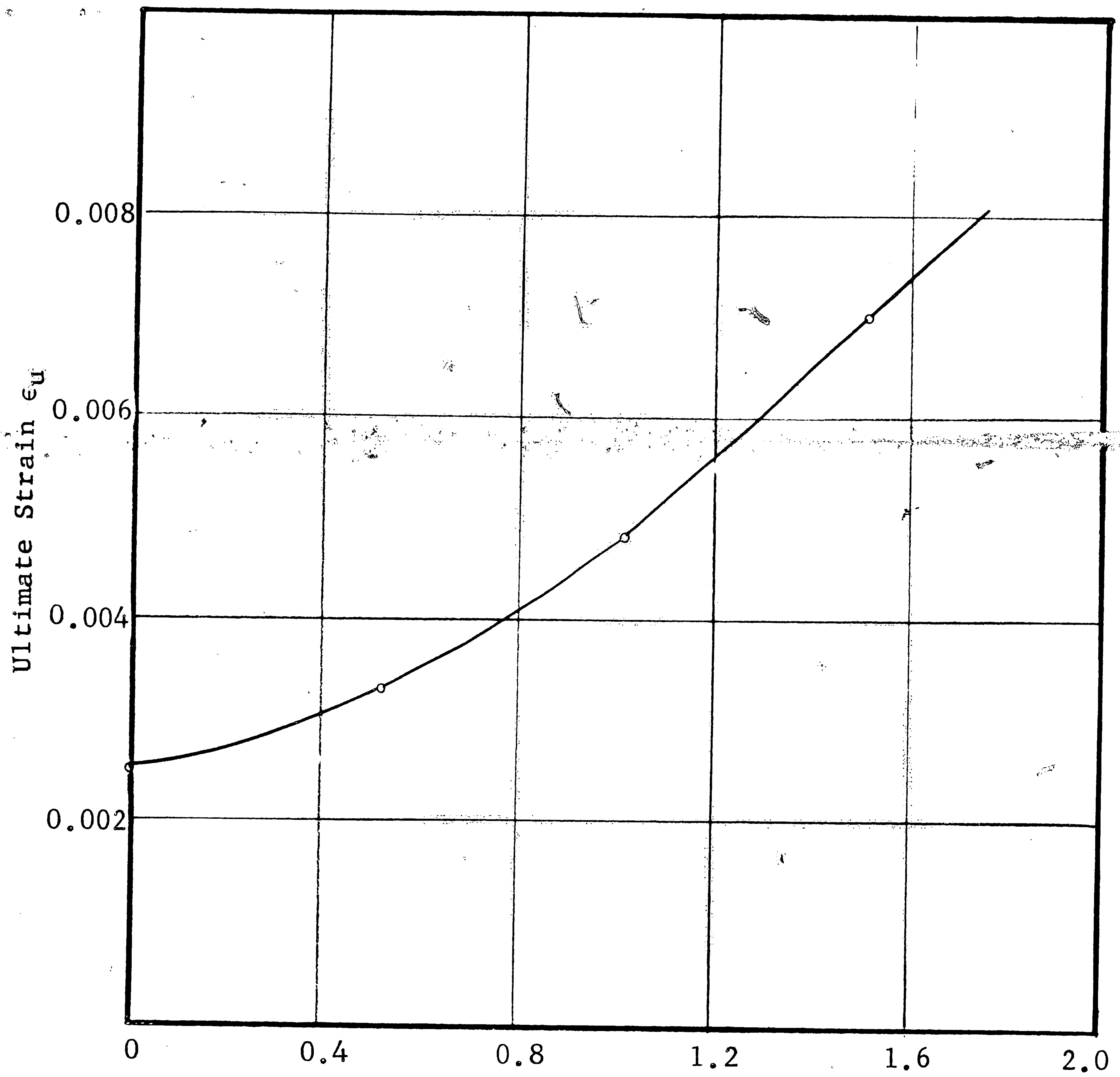

$$P_l = \frac{\text{Volume of Lateral Steel}}{\text{Volume of Total Concrete}}$$

Fig. 26 LATERAL STEEL RATIO P_l VS CONCRETE ULTIMATE STRAIN ϵ_u

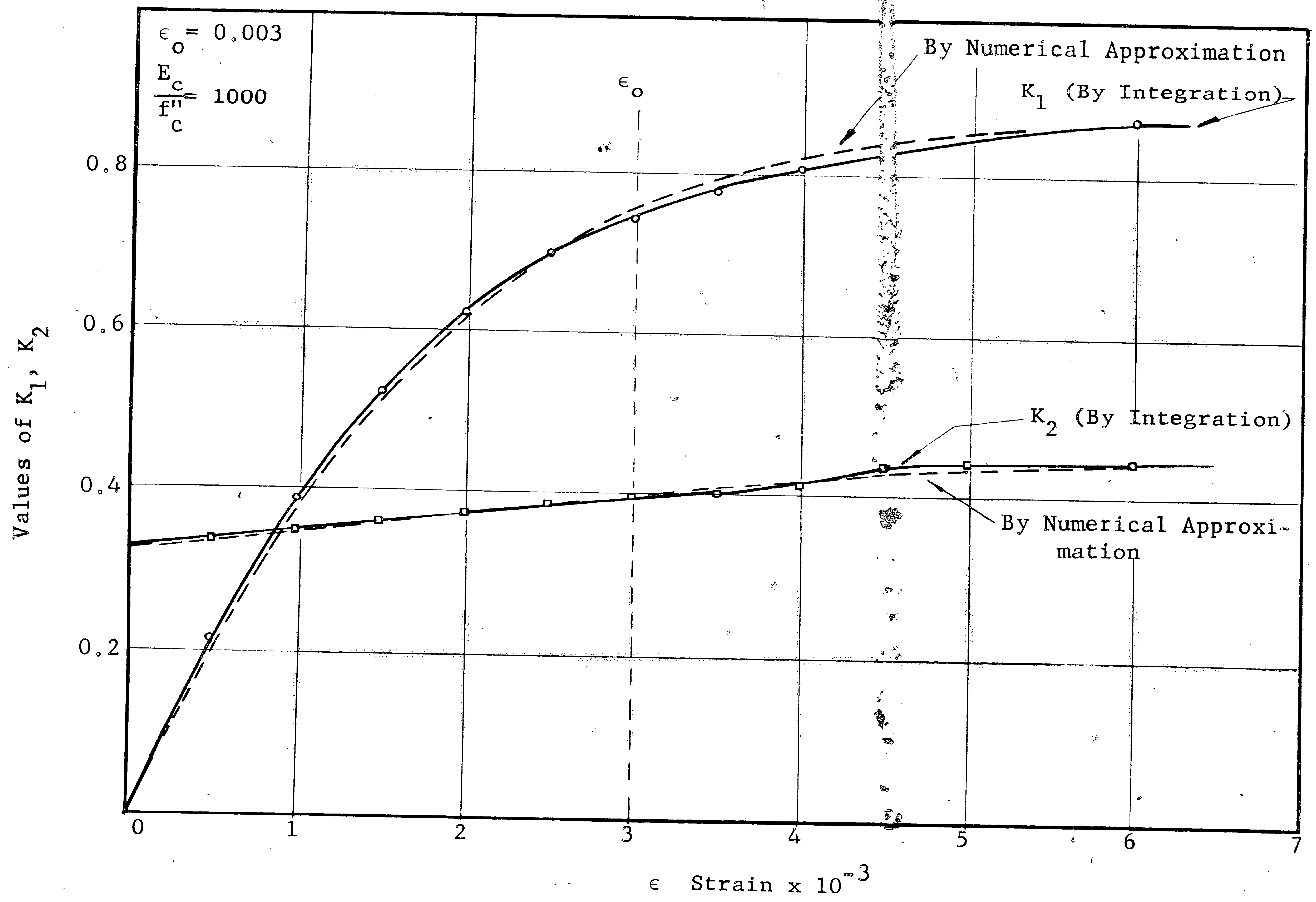

Fig. 27 CONCRETE COMPRESSIVE STRESS FACTOR K_1 AND K_2 VS ϵ_c

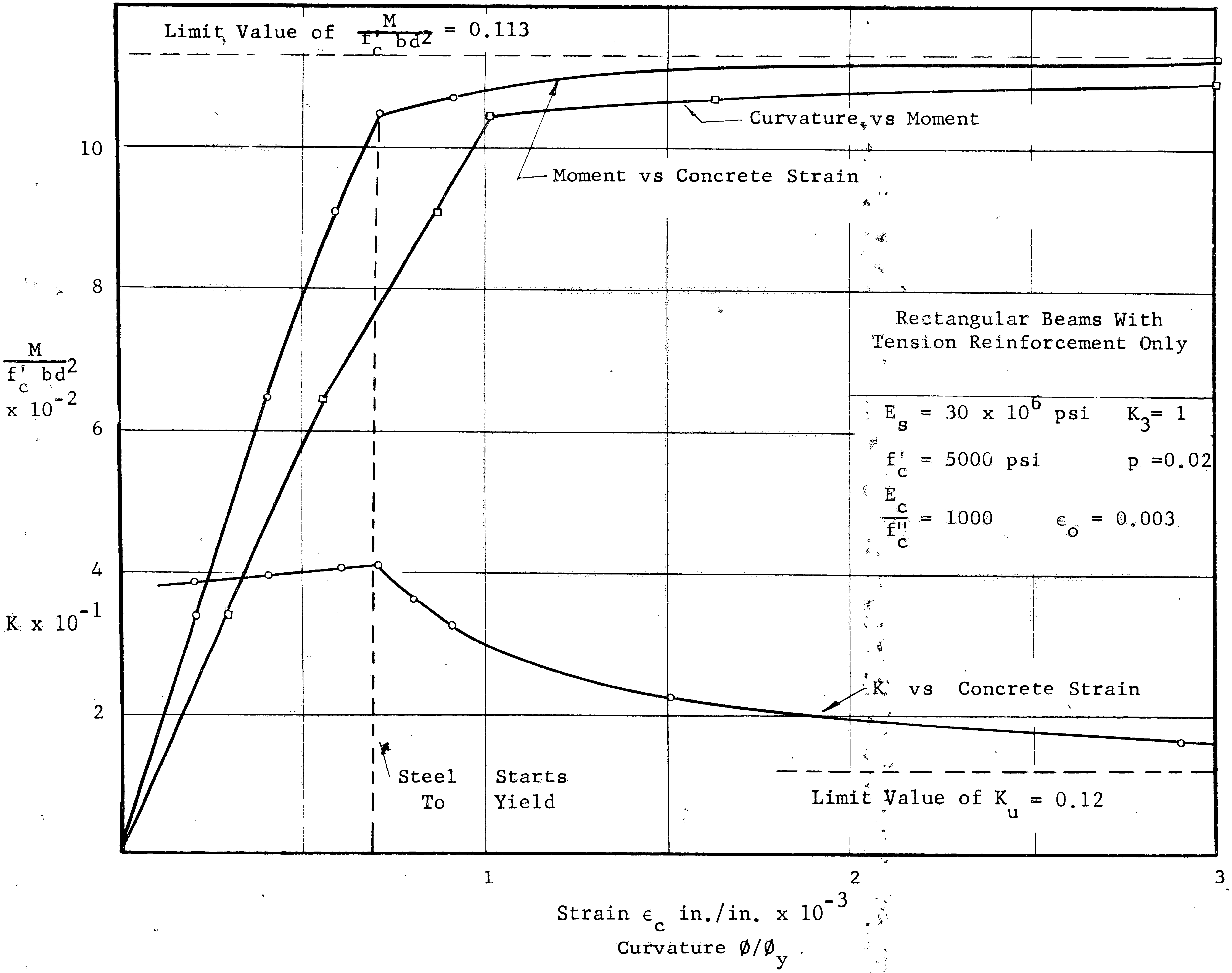

Fig. 28 $\frac{M}{f'_c bd^2}$ vs. $\frac{\phi}{\phi_y}$, $\frac{M}{f'_c bd^2}$ vs ϵ_c AND K vs ϵ_c CURVES

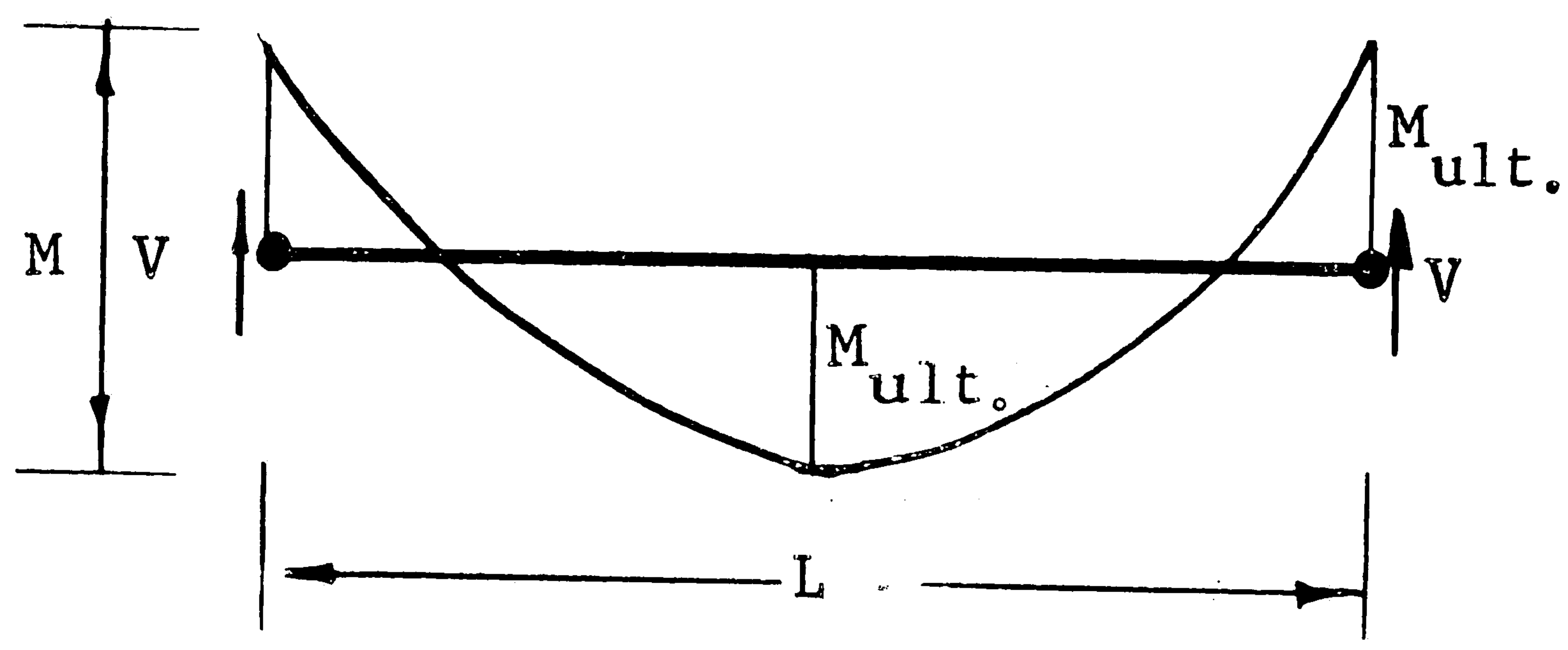

Fig. 29 PLASTIC LENGTH (EXAMPLE)
(See Appendix, section 4.4)

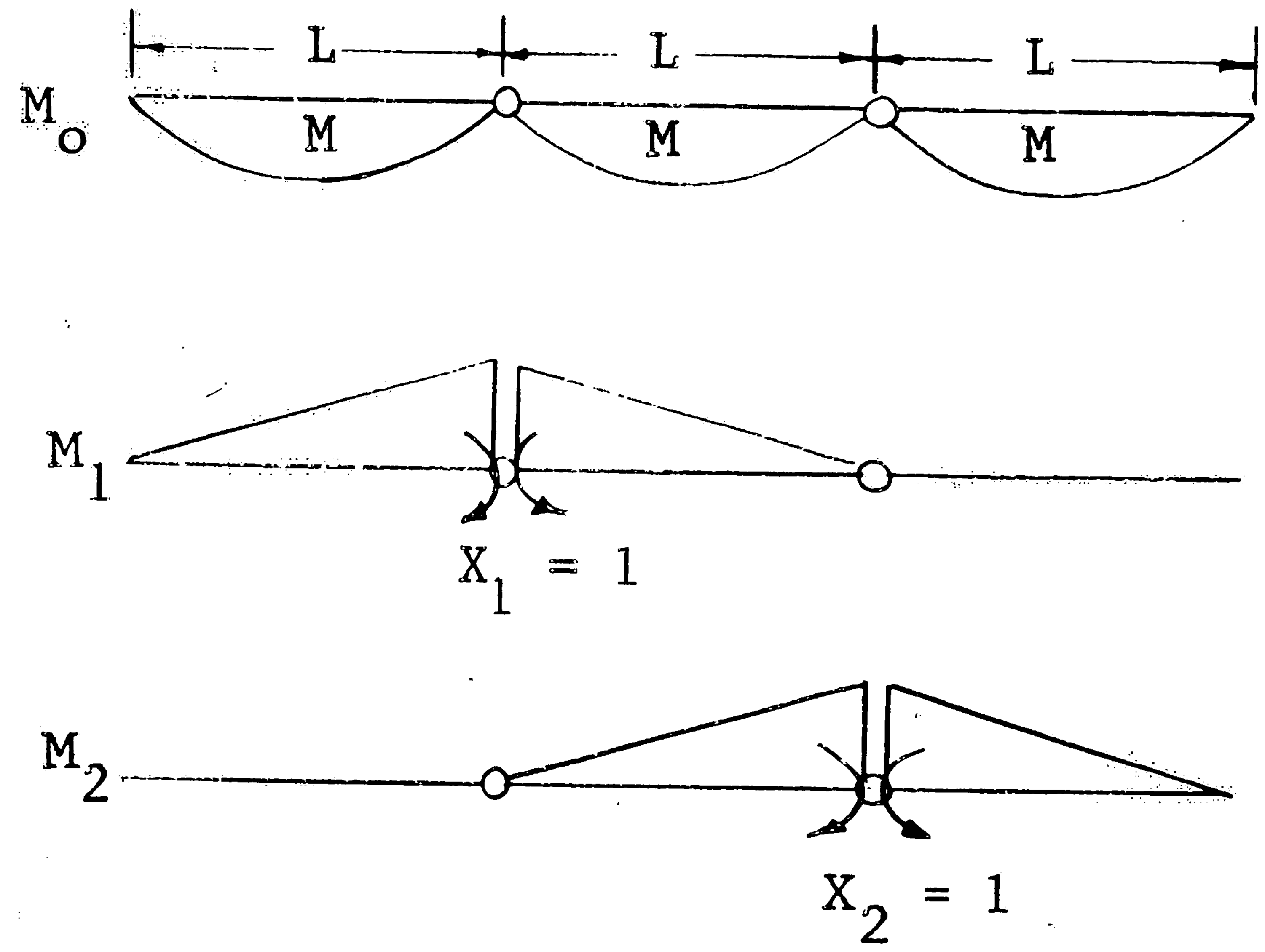

Fig. 30 CONTINUOUS BEAM (EXAMPLE)
LOAD MOMENTS AND PLASTIC-HINGE
MOMENTS (See Appendix, section 4.6)

7 REFERENCES

1. ASCE-ACI Joint Committee on Ultimate Strength Design
   REPORT OF ASCE-ACI JOINT COMMITTEE ON ULTIMATE STRENGTH DESIGN, Proceedings of the American Society of Civil Engineers, V.81, Separate No. 809, October, 1955 p.809-1 to 809-68

2. Yu, C.W. and Hognestad, E.
   REVIEW OF LIMIT DESIGN FOR STRUCTURAL CONCRETE, Proceedings of the American Society of Civil Engineers, V.84, Separate No. 1878, December, 1958

3. Beedle, L.S.
   PLASTIC DESIGN OF STEEL FRAMES, John Wiley, 1958, pp.199-204

4. Hognestad, E., Hanson, N.W., and McHenry, D.
   CONCRETE STRESS DISTRIBUTION IN ULTIMATE STRENGTH DESIGN, Journal of the American Concrete Institute, V.52, December, 1955, p.459

5. Chan, W.W.L.
   THE ULTIMATE STRENGTH AND DEFORMATION OF PLASTIC HINGES IN REINFORCED CONCRETE FRAMEWORKS, Magazine of Concrete Research, V.7, No. 21, November, 1955, pp.121-132

6. Ernst, G.C.
   A BRIEF FOR LIMIT DESIGN, Proceedings of the American Society of Civil Engineers, V.81, Separate No. 583, January, 1956, pps. 583-5 - 583-21

7. Sawyer, H.A.
   ELASTIC-PLASTIC DESIGN OF SINGLE SPAN BEAMS AND FRAMES, Proceedings of the American Society of Civil Engineers, V.81, Separate No. 851, 1955, pps. 1-29

8. Baker, A.L.L.
   THE ULTIMATE LOAD THEORY APPLIED TO THE DESIGN OF REINFORCED AND PRESTRESSED CONCRETE FRAMES, Concrete Publications, London, 1956

9. Warner, R.F.
   PROBABLE FATIGUE LIFE OF PRESTRESSED CONCRETE FLEXURAL MEMBERS, Unpublished Ph.D. Dissertation, Fritz Engineering Laboratory Report No. 223.24, Lehigh University, September, 1961

10. Newmark, N.M.
    NUMERICAL PROCEDURE FOR COMPUTING DEFLECTIONS, MOMENTS, AND BUCKLING LOADS, Transactions of American Society of Civil Engineers, V.108, Paper No. 2202, 1943, p.1161

11. Taylor, Angus E.
THE THEORY OF INTEGRATION, Advanced Calculus, Ginn & Co., 1955, pps. 519-525

12. Hognestad, E.
ULTIMATE STRENGTH OF REINFORCED CONCRETE IN AMERICAN DESIGN PRACTICE, Proceedings of a Symposium on the Strength of Concrete Structures, London, May, 1956

13. Hognestad, E.
CONFIRMATION OF INELASTIC STRESS DISTRIBUTION IN CONCRETE, Proceedings of the American Society of Civil Engineers, Proceedings Paper 1189, V.83, No. ST2, March, 1957

14. Mattock, A.H.
REDISTRIBUTION OF DESIGN BENDING MOMENTS IN REINFORCED CONCRETE CONTINUOUS BEAMS, Proceedings of the Institute of Civil Engineers, Paper No. 6314, Vol. 13, 1959, p.35

15. Kriz, L.B.
ULTIMATE STRENGTH CRITERIA FOR REINFORCED CONCRETE, Proceedings of the American Society of Civil Engineers, Proceedings Paper 2095, V.85, No. EM3, July, 1959

8. VITA

The author was born in Ching-Tien, Ckekiang, China, on December 23, 1936, the son of You-Chao and Shui-Da Chen. He entered Cheng-Kung University in September, 1955, and was awarded a Bachelor of Civil Engineering Degree in June 1959.

In September, 1961 the author joined the staff of Fritz Engineering Laboratory, Lehigh University, as a Baldwin Fellow. He was appointed to his present position of Research Assistant in Civil Engineering in 1962.